1 **Insights into the explosive eruption history of Campanian volcanoes prior to the**
2 **Campanian Ignimbrite eruption**

3 S.O. Vineberg[a*], R. Isaia[b], P.A Albert[c], R. Brown[d], V.C. Smith[a]

4 [*] *Corresponding author*
5 [a] *Research Laboratory for Archaeology and the History of Art, University of Oxford, UK*
6 [b] *Osservatorio Vesuviano, INGV, Italy*
7 [c] *Department of Geography, Swansea University, UK*
8 [d] *Department of Earth Sciences, University of Durham, UK*
9

10 **Highlights:**

11 • Twelve eruption deposits are identified between 56 ka and 40 ka indicating Ischia and
12   Campi Flegrei were very active between large caldera-forming eruptions.
13 • The three deposits from Ischia have similar glass compositions, which has implications
14   for using them and thea Schiappone ephra as marker layers.
15 • The compositions of the nine Campi Flegrei deposits can be categorised into three
16   glass chemistry groups.
17 • Glass compositions become more evolved over time, extending toward a composition
18   that is also present in the CI deposits.
19

20 **Abstract:**

21 The Campanian Volcanic Zone (CVZ) comprises multiple active volcanoes and includes the
22 highly productive Campi Flegrei and Ischia caldera systems. These caldera volcanoes have
23 produced probably the largest eruptions in Europe in the past 200 ka, such as the Monte
24 Epomeo Green Tuff (MEGT; Ischia) at ca. 56 ka and the Campanian Ignimbrite (CI; Campi
25 Flegrei) at ca. 40 ka, which form widespread isochrons traced across the Mediterranean
26 region. These closely spaced volcanic centres erupt phonolitic and trachytic glass
27 compositions that are similar, and thus it can be challenging to correlate tephra deposits to
28 specific volcanic sources. Here we present a detailed tephrostratigraphy for pre-CI eruption
29 activity using the units preserved within a sequence at the coastal Acquamorta outcrop, on
30 the western side of the CI caldera rim. Both the MEGT and CI units are present in the section,
31 and they bracket twelve eruption units that were logged and sampled. New major and trace
32 element glass chemistry data have been acquired for these Acquamorta tephra deposits.
33 Three eruption deposits from Ischia and nine from Campi Flegrei were identified, which helps
34 constrain the tempo of volcanic activity of these centres between the large caldera-forming
35 eruptions. The three Ischia tephra deposits between the MEGT and the CI are
36 indistinguishable on both major and trace element glass chemistry and cannot be correlated

to a specific known eruption in this interval, such as the Schiappone. The compositional variations between the Campi Flegrei eruptions reveal temporal shifts in the composition of the tephra deposits that reflect changes in the magmatic system prior to the CI eruption. These deposits indicate that there were at least nine eruptions from Campi Flegrei within 16 ka of the enormous CI eruption, and suggest that there was no significant period of repose before the caldera generating eruption.

Key words: *Tephrostratigraphy, Campi Flegrei, Ischia, Volcanism, Volcanic glass chemistry, Eruption records, Magmatic systems*

1. Introduction

Records of past volcanism reveal the magnitude, frequency, tephra dispersal and how magma systems have evolved over time. Near-vent (proximal) eruption sequences are fundamental to the reconstruction of past volcanic histories by providing stratigraphic, chronological and geochemical constraints. However, proximal outcrops near volcanoes, especially caldera systems that have produced large explosive eruptions (i.e. those with volcanic explosivity index (VEI) ≥6; Newhall and Self, 1982) are often destroyed and/or buried by voluminous eruption deposits. As a result, only fragmentary eruption records are typically preserved or accessible at sites around the vent (Fig. 1). Distally located sedimentary archives (e.g. lacustrine, marine cores) overcome such preservation and accessibility issues and often contain more tephra deposits associated with small and medium sized eruptions than their proximal counterparts (e.g. Wulf et al., 2004, 2008; Bourne et al., 2010; Wutke et al., 2015; Giaccio et al., 2017). The absence of such deposits being recognised in the proximal record does not allow precise correlations in medial and distal areas as the information on the number, frequency and full geochemical range of eruptions are poorly constrained and consequently affect both the reconstruction of the volcanic history and the tephrochronological framework of the mid-distal proxy.

The Campanian Volcanic Zone (CVZ) consists of four volcanoes: Campi Flegrei (Phlegraean Fields), Ischia, Procida and Somma-Vesuvius (Fig. 2a), which have experienced explosive activity throughout the Late Pleistocene. Both Ischia and Campi Flegrei have produced caldera-forming eruptions in the last 100 ka, with at least three large magnitude eruptions from the Campi Flegrei volcano: the Campanian Ignimbrite (CI, 39.9 ± 0.1 ka; Giaccio et al., 2017), the largest eruption in Europe for the past 200 ka; the Masseria del Monte Tuff (MdMT, 29.3 ± 0.7 ka; Albert et al., 2019), that corresponds to the widespread Y-3 marker layer (e.g. Keller et al., 1978); and the Neapolitan Yellow Tuff (NYT, 14.2 ± 0.2 ka; Bronk Ramsey et al., 2015). Ischia produced the caldera-forming Monte Epomeo Green Tuff (MEGT;

1   Brown et al., 2008) at 56.1 ± 1.0 ka (Giaccio et al., 2017). These four tephra units form key
2   chronostratigraphic markers and have aided in the synchronisation and chronology of Late
3   Pleistocene sedimentary sequences across the central Mediterranean region (e.g. Schmidt et
4   al., 2002; Fedele et al., 2003; Wulf et al., 2004, 2012, 2018; Bourne et al., 2010; Albert et al.,
5   2015; Giaccio et al., 2017). These marker units are prominent around the calderas, but tephra
6   deposits from eruptions preceding these events are not well exposed in proximal regions.
7   Thus, the eruption history within the CVZ is not well constrained in the periods leading up to
8   these voluminous eruptions.

9   Deposits from CVZ eruptions preceding the CI eruption are present in both proximal
10   and distal tephra sequences. However, the number of eruptions and their timing is poorly
11   constrained. Deposits separated by paleosols under the CI occur along the caldera wall faults
12   (e.g. Rosi et al., 1987; Orsi et al., 1996; Pappalardo et al., 1999; De Vivo et al., 2001; Di Vito
13   et al., 2008). Research on tephra sequences across the Campanian Plain reveal numerous
14   tephra deposits including two key Late Quaternary (Marine Isotope Stage; MIS 5e) central
15   Mediterranean tephrostratigraphic markers (the X-5 and X-6 tephras), however there is a
16   paucity of deposits between 90 ka and 40 ka (see: Monaco et al., 2022; Donato et al., 2016;
17   Giaccio et al., 2012). Furthermore, the sediment core from Lago di Monticchio (LGdM; Fig. 2b)
18   is a valuable record of explosive volcanism in Italy, with at least nine tephra deposits between
19   the MEGT and CI which are attributed to pre-CI Campi Flegrei and Ischia events based on
20   geochemical evidence (see: Wulf et al., 2004, 2008; Wutke et al., 2015). The lack of
21   geochemical data for the pre-CI units in proximal sectors prevents correlations of distal tephras
22   to proximal pre-CI deposits. As such, many pre-CI distal tephra deposits have not yet been
23   ascribed to a particular proximal equivalent (e.g. Munno and Petrosino, 2007; Wulf et al., 2012;
24   Giaccio et al., 2017). Such uncertainties surrounding the origins and incompleteness of
25   geochemical characterisation of these pre-CI units inhibits their use for any volcanological
26   purposes and limit their tephrochronological potential.

27   Here we address this knowledge gap by focussing on a sequence located on the
28   western side of the CI caldera wall that is exposed between the MEGT and CI. In this research
29   we present stratigraphic descriptions of the deposits and their glass chemistry and then use
30   this geochemical data to assess tephra correlations across the southern Mediterranean.

31

2. Campanian volcanic centres and eruptions prior to the Campanian Ignimbrite

33   All CVZ volcanoes have been active over the past 100 ka, dispersing tephra across
34   the Mediterranean and beyond (e.g. Orsi et al., 1996; Brown et al., 2007; Bourne et al., 2010;
35   Tomlinson et al., 2014; Smith et al., 2016). The CVZ volcanoes produce similar glass

1   compositions but the specific volcanic source can be identified. Useful elements (e.g. CaO,

2   Na_2O, Na_2O/K_2O, Nb, Th, Zr/Sr) and bivariate plots (e.g. CaO vs SiO_2, MgO vs CaO,

3   Na_2O/K_2O vs CaO, Y vs Th, Zr/Sr vs Th) that help differentiate the volcanic source for trachytic

4   to phonolitic tephra from the CVZ volcanoes are outlined in Tomlinson et al. (2015) and

5   Giaccio et al. (2017). Whilst the Somma-Vesuvius volcano is part of the CVZ, there are no

6   explosive deposits recorded prior to the Pomici di Base eruption at 22.1 ± 0.4 ka (Cioni et al.,

7   1999; Bronk Ramsey et al., 2015) and thus we do not consider it as a potential source for

8   these tephra deposits presented in this study.

9

10   ### 2.1 Campi Flegrei

11   Campi Flegrei is the largest volcano in the CVZ, and it hosts a 13 km wide nested caldera

12   which encompasses the outskirts of the city of Naples and extends beneath the Gulf of

13   Pozzuoli (see: Fig. 2a). The earliest eruptions ascribed to this volcanic system include the

14   three Seiano Ignimbrites (290 – 240 ka), the Taurano Yellow Tuff (~157 ka) and the Durazzano

15   Ignimbrite (~116 ka; De Vivo et al., 2001; Rolandi et al., 2003). Medial outcrops on the

16   Campanian Plain (Di Vito et al., 2008) and Sorrento Peninsula (De Vivo et al., 2001; Rolandi

17   et al., 2003) record tephra deposits from at least seven eruptions which, based on stratigraphic

18   and geochemical data, have been linked to Campi Flegrei and were erupted between 290 and

19   110 ka (Fig. 2a). Four of these units (Triflisco, Santa Lucia, Cancello, and Maddaloni)

20   preserved within the foothills of the Apennine Mountains, 60 km east of Campi Flegrei (Fig.

21   2a), were erupted 110 – 90 ka (Fig. 1; Monaco et al., 2022). The nested caldera was generated

22   and modified during the CI, MdMT and the NYT eruptions at 40 ka, 29 ka and 14 ka,

23   respectively. There have been >70 eruptions within the caldera since the NYT (e.g. Di Vito et

24   al., 1999; Orsi et al., 2004; Isaia et al., 2009; Smith et al., 2011). Details on the activity in the

25   26 ka period between the CI and NYT eruptions is limited with only a few sections logged (Orsi

26   et al., 2004; Albert et al., 2019).

27   Some proximal sections reveal tephra deposits below the CI eruption. Eleven separate

28   units are seen beneath the CI at Trefola, three at Torre di Franco and one at both Cuma and

29   San Severino (see: Fig. 2a). Many of the pre-CI units have not been characterised with some

30   whole-rock data on a selection of units (Pappalardo et al., 1999; Pabst et al., 2008; Giaccio et

31   al., 2017), and limited glass data (Tomlinson et al., 2012).

32

33   ### 2.1.1 Compositions of pre-CI Campi Flegrei tephra

34   The chemical composition of the older pre-CI Campi Flegrei glasses range from high-K

35   phonolites to trachytes. They are moderately to highly evolved and characterised by their low

SiO$_2$ and high CaO, FeO$_t$ and Al$_2$O$_3$ concentrations relative to the CI and show decreasing CaO, FeO$_t$ and Al$_2$O$_3$ with increasing SiO$_2$ (see: Tomlinson et al., 2012; Giaccio et al., 2017). Many of the successive tephra units have overlapping major and trace element glass compositions, which means it is difficult to differentiate the deposits (Tomlinson et al., 2012, 2015; Wutke et al., 2015). Proximal pre-CI Campi Flegrei deposits are studied in the most detail at Trefola, with only XRF whole-rock data of only a selected number of tephra units from the sequence (see Fig. 2a). Three compositional clusters have been identified for these pre-CI Campi Flegrei deposits based on the available XRF and isotope data for selected deposits (see: Pappalardo et al., 1999; Pabst et al., 2008.) The TLa and TLc units are defined as Pre-CI Group 1; TLf, to TLi units defined as Pre-CI Group 2; and the TLm unit defined as Pre-CI Group 3 (Pabst et al., 2008). Glass from the TLa, TLc, and TLf units have been analysed and they show that incompatible element enrichment in these units decreases with time (TLa>TLc>TLf; Tomlinson et al., 2012), and their glass compositions are different to those documented after the large CI and NYT eruptions (e.g. Pappalardo et al., 1999; Di Renzo et al., 2011; Smith et al., 2011; Forni et al., 2018).

2.1.2 Distal records of Campi Flegrei tephra (Pre-CI)

Sedimentary records across the central Mediterranean reveal at least fourteen Campi Flegrei derived distal eruption deposits between ~65 ka and the CI. The varved (annually laminated) LGdM sediment record, 90 km east of the CVZ, contains numerous tephra and cryptotephra deposits (termed the TM-18 tephras; Fig 2b) between the MEGT (TM-19) and the CI (TM-18), making it a key record of pat volcanism in the CVZ (Wulf et al., 2004; 2018; Wutke et al., 2015). Four tephra (TM-18-1a-d) were deposited within 600 varve years of the CI at LGdM, and they show a very strong geochemical affinity with Campi Flegrei products and the glass compositions of the CI (see: Wutke et al., 2015). Of these tephras, Wulf et al. (2018) identify the compositionally distinct, 1 cm thick, grey-brown TM-18-1d tephra as the most useful marker, as glass compositions show decreased SiO$_2$ compared to the other (TM-18-1a-c) deposits and display more enriched incompatible element contents (Th, 53-89 ppm; U, 21-33 ppm; Nb, 131-198 ppm; Zr, 681-1072 ppm).

The lacustrine record of Fucino, 130 km north of Campi Flegrei, contains one tephra layer preserved between the MEGT and CI (TF-6; Fig. 2b), which is tentatively correlated to the TLc unit at Trefola based on stratigraphic, chronological and geochemical data (Giaccio et al., 2017). The Tenaghi Philippon sequence on mainland Greece, 675 km east of Campi Flegrei, contains six cryptotephra deposits preserved within the 1.25 m sediments beneath the CI, corresponding to 40.1 – 46.7 ka cal. BP (Wulf et al., 2018). Here the LGdM TM-18-1d

1   has been tentatively identified as a cryptotephra (TP05-13.34; Wulf *et al.*, 2018). The

2   remaining five cryptotephra deposits (TP05-13.25, TP05-13.28, TP05-13.54, TP05-13.92 and

3   TP05-14.50) at Tenaghi Philippon (Fig. 2b), and pre-CI two cryptotephra deposits (IO8T-30.74

4   and IO8T-31.17) identified between 0.6 – 1m below the CI at Ioannina (Greece), located 450

5   km east of Campi Flegrei (Fig. 2b), show geochemical similarities with the LGdM TM-18-1a-c

6   tephras and the CI (see: Wulf et al., 2018; McGuire et al., 2022). All seven of the Tenaghi

7   Philippon cryptotephra deposits were interpreted to reflect down core remobilisation of CI

8   glasses due to their overlapping geochemical data with the CI, despite both showing discrete

9   peaks in shard concentration relative to background concentrations almost 2 m below the CI

10   tephra. Further work on the proximal sections can reveal whether the similar chemistries of

11   successive units at these distal sites reflects reworking or different eruptions of compositionally

12   similar magmas.

13

14   ### *2.2. Ischia*

15   Ischia is the most westerly of the CVZ volcanoes, located on the same NE-SW trending fault

16   system as the Campi Flegrei volcano (Fig. 2a), and is thought to represent the remnants of a

17   larger volcano (Santacroce et al., 2003; Orsi et al., 2004). The eruption history of Ischia is

18   documented back to ~150 ka (Poli et al., 1987) and has been active into historical times with

19   the latest eruption in 1302 CE. Volcanic activity has been divided into five phases: >150-75

20   ka; 75-55 ka; 55-33 ka; 28-12 ka; 12 ka-1302 CE (Poli et al., 1987; Brown et al., 2008). The

21   55-33 ka phase of activity is characterised by several explosive events including the MEGT

22   (Poli et al., 1987) that occurred at ~56 ka and resulted in caldera collapse across all or part of

23   the island (Buchner, 1996; Vezzoli 1988; Civetta et al., 1991; Orsi et al., 1991; Brown et al.,

24   2008). The widespread Y-7 tephra marker, traced as far as the Ionian Sea, has been

25   correlated with the MEGT eruption (Tomlinson et al., 2014), but this has been disputed based

26   on mineral compositions (D'Antonio et al., 2021). The proximal outcrops on the island of Ischia

27   preserve the deposits of at least six explosive eruptions between the MEGT and CI, while a

28   further five units have been identified below the MEGT (Fig. 1).

29

30   ### *2.2.1 Compositions of pre-CI Ischia tephra*

31   Glass compositions of tephra from Ischia are phono-trachytic in composition and show minor

32   overlap with Pre-CI Campi Flegrei/CI tephra deposits (see: Tomlinson et al., 2014). Pre-MEGT

33   tephra deposits are characterised by low CaO, and high SiO_2 and Na_2O relative to the MEGT,

34   with a trend of decreasing Na_2O and FeO_t with increasing K_2O (Tomlinson et al., 2014, 2015).

35   The studied Ischia glasses have a wide range of incompatible trace element concentrations,

1   and extend to highly enriched concentrations (e.g. Zr ranging from 160 to 1110 ppm;

2   Tomlinson *et al.,* 2014) that are characterised by high Zr/Sr ratios (up to 670; Tomlinson et al.,

3   2015). There is a significant change in the composition of Ischia tephras prior to and following

4   the caldera-forming MEGT eruption (Tomlinson *et al.,* 2015). Relative to pre-MEGT and MEGT

5   glasses, post-MEGT deposits are displaced to lower MgO, FeO_t, TiO_2 and incompatible

6   element contents (Tomlinson et al., 2014). Nevertheless, despite the Ischia eruption

7   stratigraphy being better resolved than that for Campi Flegrei, glass geochemical data is still

8   lacking for several post-MEGT tephra units (e.g. the Chiammano, La Roia and Capo Grosso

9   tephras; Fig.1).

10

2.2.1 Distal pre-CI Ischia tephra

12   Medial to distal records from across Italy preserve at least eleven tephra deposits from Ischia

13   between the CI and MEGT in both marine and terrestrial sequences. Five pre-CI Ischia tephra

14   deposits have been identified in marine cores (Fig. 2b), one being a cryptotephra deposit from

15   the Adriatic Sea (PRAD-1752; Bourne et al., 2010) and four visible tephra deposits the

16   Tyrrhenian Sea (C-14, C-15, C-16 and C-17; Paterne et al., 1986, 1988). The SMP1-a fallout

17   deposit preserved beneath the CI on the Sorrento Peninsula (Fig. 2a) has been correlated to

18   Ischia based on XRF data (Di Vito et al., 2008). Furthermore, the tephra deposit in the Adriatic

19   Sea (PRAD-1752) and SMP1-a tephra have been correlated with the LGdM TM-18-1 tephra

20   (Wutke et al., 2015). However, neither the specific stratigraphic position within the LGdM

21   sequence nor geochemical data has been published for the TM-18-1 tephra and therefore, it

22   is not discussed further in this study.

23   A further thirteen Ischia tephra deposits are reported between 104 and 40 ka in the

24   LGdM record (Tomlinson et al., 2014), including the distal equivalent of the MEGT (TM-19;

25   Wulf et al., 2004). Five of these LGdM deposits are preserved between the MEGT and CI (TM-

26   18-2, TM-18-9a, TM-18-9e, TM-18-14a and TM-18-17a; Tomlinson et al., 2014), and of these

27   markers, Wulf et al. (2018) identify the TM-18-14a and TM-18-9e tephras as the most useful

28   marker horizons due to their distinctive geochemical compositions relative to the other Ischia

29   deposits in the sequence. Two of these LGdM tephra deposits have been correlated to the

30   Schiappone (TM-18-17a) and the Pietre Rosse (TM-18-14a) eruption units (Tomlinson et al.,

31   2014). The LGdM TM-18-17a glasses are compositionally variable (61.7 – 62.8 wt.% SiO_2, 13

32   – 24 ppm Th and 204 – 360 ppm Zr) and show a complete overlap with the proximal

33   Schiappone tephra with the dominant population of the glass compositions lying within the

34   least evolved member (Fig. 5e–f; Tomlinson et al., 2014). Furthermore, the whole rock

35   chemical data presented by Paterne et al. (1986, 1988) for the C-16 tephra preserved in

multiple cores from the Tyrrhenian Sea show highly variable glass compositions and some that overlap with the most evolved Schiappone glasses (Tomlinson et al., 2014). Whilst the marine C-17 Ischia tephra also displays geochemical similarities with the TM-18-17a glasses, the whole rock data for the C-17 deposit extends to higher (~1) K_2O/Na_2O and lower (0.67 – 0.91 wt.%) CaO values (Tomlinson *et al.*, 2014). Therefore, the TM-18-17a and C-16 tephra marine deposits are believed to be distal correlatives of the Schiappone Tephra (Tomlinson et al., 2014). A re-assessment of the glass chemistry of the Tyrrhenian Sea Ischia layers is required to verify correlations.

The three remaining Ischia deposits between the MEGT and CI in the LGdM core have not been correlated to specific eruptions. Whilst the LGdM TM-18-9e tephra shares geochemical similarities with the proximal Agnone deposit, the CaO is much lower (up to 30% lower; Tomlinson et al., 2014). Although the post-MEGT LGdM TM-18-9a tephra is a moderately evolved (Zr 335 – 454 ppm; Th 22 – 32 ppm), it is compositionally between the Agnone and Pietre Rosse deposits and does not correlate with any known proximal eruption unit (Tomlinson et al., 2014). The youngest pre-CI LGdM Ischia tephra (TM-18-2) has tentatively been correlated to the C-14 Tyrrhenian Sea tephra based on whole rock XRF compositions (Wutke et al., 2015).

2.3. Procida

The Island of Procida sits between Ischia Island and Campi Flegrei in the Gulf of Pozzuoli, (Fig. 2a). It is comprised of overlapping, eroded edifices of five monogenic explosive eruptions: Vivara, Terra Murata, Pozzo Vechio, Fiumicello and Solchaiario (Rosi et al., 1988). Procida has been active from ~80 ka until the Solchario eruption (De Astis et al., 2004), which, based on ^{14}C ages from paleosols below and above the unit, has an eruption age of 23,005-24,201 cal yrs BP (19,620 ± 270 yrs BP; Alessio *et al.,* 1976). Little geochemical or chronological data is available for units preceding the Solchario eruption.

The interbedding of pyroclastic deposits on Procida with those from Campi Flegrei and Ischia has provided stratigraphic and chronological constraints on some of the eruptions (Fig. 1). Two units, Vivara I and the younger Fiumicello, occur below the MEGT indicating that they erupted pre-56 ka; and the Vivara II deposit sits between the MEGT and the CI (Fig.1: De Astis et al., 2004). No Procida tephra deposits between the MEGT and CI have been identified in distal settings. Whole rock data for the pre-CI Fiumicello and post-CI Solchiaro eruptions indicates both are trachybasaltic (Rosi et al., 1988; Scandone et al., 1991).

3. Study Site

This study aims to improve the pre-CI (<40 ka) eruption history by reconstructing a detailed proximal tephrostratigraphy for pre-CI eruption activity through visual description and geochemical characterisation. We utilise a coastal outcrop at Acquamorta, also referred to as Monte di Procida (see: Rosi et al., 1988; Orsi et al., 1996; Perrotta et al., 2010), on the west side of the CI caldera ring fault (40° 47'39.8" 014° 02' 37.2"; Fig 2a), 14 km from Ischia and 5 km from Procida.

Numerous pyroclastic deposits beneath the CI were previously noted at Acquamorta and nearby Torregaveta (e.g. Rosi et al., 1988; Orsi et al., 1996) and thought to be from multiple volcanic sources (Campi Flegrei, Procida and Ischia). However, the number of units extending from the base of the sequence up to the CI differs between publications; Rosi et al. (1988) observed six units, Orsi et al., (1996) identified five units, and Perrotta and Scarpati (1994) noted four units. None of these previous studies presented details of the units or any compositional analyses. A >0.5 m thick green-grey coarse pyroclastic density current (PDC) deposit, the base of which is not exposed, outcrops at Acquamorta. This has been correlated to the MEGT eruption using glass chemistry (see: Tomlinson et al., 2014). The Fiumicello tephra from Procida, a 1.3 m thick distinctively grey bedded unit, outcrops below the MEGT (Rosi et al., 1988; De Astis et al., 2004; Perrotta et al., 2010) and to the left (north) of the section that we sampled (Fig. 3a). These pre-MEGT units are behind concrete or metal netting and higher up in the section. These units dip below the beach at the section that we sampled so that only the units between the MEGT and the CI are accessible; consequently, this study focusses on these eruption deposits.

4. Methods

4.1. Eruption stratigraphy

The Acquamorta outcrop was logged and sampled during field campaigns in 2013, 2014 and 2021. Representative samples were collected for geochemical characterisation. Paleosols have allowed numerous eruption units to be defined, which have been given a number and AQ prefix. Samples for geochemical analysis were given a number and CF prefix.

4.2. Glass chemistry

In the laboratory, bulk representative samples comprising of pumice clasts and ash were crushed and wet sieved to remove the fraction less than 80 μm. Samples were dried in an oven at ~ 60°C and mounted in epoxy for analysis.

1   Major element glass compositions of the samples were analysed using a JEOL-8600

2   and a JEOL JXA-8200 wavelength dispersive electron microprobe (WDS-EMP) equipped with

3   5 spectrometers located in the Research laboratory for Archaeology and the History of Art

4   (RLAHA), University of Oxford, U.K. To minimise alkali-loss in the glass, an accelerating

5   voltage of 15 kV, a 6 nA beam current and a beam diameter of 10 μm were used. Peak

6   counting times were 12 s for Na, and other major elements collected for 30 s except for Mn,

7   Cl and P which were collected for 50 s. Background counts were collected for the same total

8   amount of time as those on peak, with half the time either side of the peak. The instrument

9   was calibrated with mineral standards and the calibration was checked with the MPI-DING

10   references glasses including the evolved felsic [ATHO-G (rhyolite)], through intermediate

11   [StHs6/80-G (andesite)] to mafic [GOR128-G (Komatiite)] glasses (Jochum et al., 2006). Due

12   to variable secondary hydration of glasses (e.g. Shane et al., 2008), all the analyses presented

13   in the text, tables and graphs have been normalised to 100% for comparative purposes.

14   Analyses with analytical totals <94% were discarded as they are not thought to be

15   representative of the melt composition. Error bars on plots represent reproducibility, calculated

16   as 2 standard deviations of replicate analyses of MPI-DING StHs6/80-G glasses.

17   The trace element compositions of individual glass shards in selected tephra units

18   were determined using an Agilent 8900 triple quadrupole LA-ICP-MS (laser ablation

19   inductively coupled plasma mass spectrometry; ICP-QQQ) coupled to a Resonetics 193 nm

20   ArF excimer laser-ablation device in the Department of Earth Sciences, Royal Holloway,

21   University of London. The full analytical procedures adopted for volcanic glass analysis follow

22   those outlined in Tomlinson et al. (2010). A range of crater sizes were used (20, 25 and 34

23   μm) owing to variability in the sample's vesicularity and thus the size of glass surfaces

24   available for analysis (see: Supplementary Material). The laser energy density on the target

25   was 3.0 Jcm^{-2}, the repetition rate was 5 Hz. The analyses comprised a count time of 40 s on

26   the sample, and 40 s on the gas blank to allow the subtraction of the background signal.

27   Typically, blocks of eight glass shards and one MPI-DING reference glass were bracketed by

28   the NIST612 glass adopted as the calibration standard. The internal standard applied was ^{29}Si

29   (determined by EMP-WDS analysis). In addition, MPI-DING reference glasses were used to

30   monitor analytical accuracy (Jochum et al., 2006). LA-ICP-MS data reduction was performed

31   in Microsoft Excel, as described in Tomlinson et al. (2010). Accuracies of LA-ICP-MS analyses

32   were monitored using MPI-DING reference glasses, ATHO-G and StHs6/80-G, and

33   accuracies were typically ≤6% for the majority of elements measured. For consistency with

34   EMP error reporting, error bars on plots show 2 times the standard deviation of replicate

35   analyses of MPI-DING StHs6/80-G. All major and trace element data are available in the

36   Supplementary Material.

1

5. Results

5.1. Pre-CI eruption stratigraphy

Twelve units separated by paleosols were identified in a 6 m succession between the MEGT and the CI at Acquamorta (Fig. 3a). The units vary in thickness, grain size and colour, and each had a sharp basal contact (Fig. 3b-f). The tephra deposits in this record at Acquamorta are relatively thin despite the proximity to the sources, suggesting that it was not on the main dispersal axis for the eruptions or that deposits are not well preserved. The prevailing wind is to the east, with very few eruption deposits preserved on the western side of the caldera; even the Plinian phase of the CI eruption is not preserved at Acquamorta. Clasts vary in colour (white-grey to brown-black), vesicularity and crystal content even within a single eruption deposit. Glass shard morphologies show little variation between the units with a range in vesicularity and microlite abundance across the units. Backscattered electron images reveal clasts of some units (for instance AQ-8) are poorly vesiculated with small (<25 µm) round vesicles. While the AQ-12 unit has large glass shards with highly abundant large vesicles (>200 µm) making it distinct from any other unit analysed in this study (see: Supplementary Material).

5.2. Glass geochemistry

Sixteen samples from the twelve tephra units were geochemically analysed. Representative major and trace element analyses are reported in Table 1. All twelve units are alkalic and straddle the phonolite-trachyte boundary (Fig. 4a). There is a wide compositional range in the major element compositions of the units spanning the entire investigated sequence, with, 58.83 – 63.23 wt.% SiO_2, 6.10 – 8.73 wt.% K_2O, 5.33 – 7.83 wt.% Na_2O, 1.23 – 2.23 wt.% CaO, 1.79 – 3.60 wt.% FeO_t ($n = 453$). Trace element compositions display a range of concentrations: 2.8 – 77.6 ppm Sr, 345 – 1001 ppm Zr, 53.5 – 185 ppm Nb, 32.1 – 77.3 ppm Y, 51.1 – 116 ppm Nd, and 24.6 – 79.4 ppm Th ($n =121$). There is little heterogeneity within individual units (i.e. similar to analytical uncertainty). Unit AQ-6 shows the greatest degree of variability in major elements (Fig. 4a-d), and unit AQ-13 showing the greatest variability in trace element concentrations (Fig. 4e-f). On the basis of the major element data, it is possible to recognise four compositional groups (see: Fig. 4a-f). These groups also have different trace element compositions. Here we highlight the key compositional features that allow the discrimination of these groups, and thus the diagnostic chemistry that can be used to aid correlations.

1   Group A includes the following three units: AQ-5, AQ-8 and AQ-11 and is dominated
2   by glass populations which firmly fall within the trachytic compositional field (Fig. 4a). This
3   group of glasses (*n=71*) are tightly clustered and are characterised by the highest SiO_2 (62.65
4   ± 0.47 wt.%) and lowest Al_2O_3, (18.65 ± 0.34 wt.%), CaO (1.38 ± 0.14 wt.%) and FeO_t (2.34 ±
5   0.29 wt.%) contents. The Group A glasses plot separately from all other units analysed at
6   Acquamorta and can most easily be separated using SiO_2 vs. Na_2O and SiO_2 vs. K_2O plots
7   (Fig. 4c,d). In terms of trace element contents (*n = 41*), the Group A tephra units possess the
8   lowest Th (29.5 ± 3.99 ppm), Nb (69.3 ± 9.21 ppm), Nd (64.5 ± 7.99 ppm) and Zr (426 ± 55.66
9   ppm) and higher Zr/Th (14.4 ± 0.83) and Y/Th (1.40 ± 0.08) relative to the other three
10   compositional groups identified at Acquamorta (Table 1). Group A can be easily separated
11   using Th vs. Y and Th vs. Nd from the three other groups (Fig. 4e,f)

12   In contrast, Groups B, C and D are dominated by phonolitic glass components and
13   show varying degrees of overlap in both major and trace element data (Fig. 4). Nonetheless,
14   they can be separated on using specific major elements, particularly unit-to-unit variations in
15   K_2O and Na_2O content (Fig. 4c-d).

16   Glasses from AQ-2 and AQ-3, directly above the MEGT (Fig.3), form Group B, and
17   display only minor overlap in both major and trace elements (Fig. 4). These glasses (*n = 85*)
18   are characterised by higher CaO (2.06 ± 0.13 wt.%) and K_2O (8.07 ± 0.37 wt.%) and lower
19   SiO_2 (59.52 ± 0.69 wt.%) and Na_2O (5.94 ± 0.45 wt.%) contents relative to units in Groups C
20   and D, and as such can easily be distinguished using SiO_2 vs. CaO, SiO_2 vs. Na_2O and SiO_2
21   vs. K_2O plots (Fig 4b-d). Whilst trace element contents (*n = 26*) are lower in Th (43.1 ± 4.56
22   ppm), Nd (73.7 ± 5.57 ppm), Y (46.1 ± 3.73 ppm) and Zr (552 ± 50.4 ppm), they show a slight
23   overlap with both Group C and D, yet they can be most easily be distinguished by their lower
24   Zr/Sr ratio (17.4 ± 7.02).

25   The five units, AQ-4, AQ-6, AQ-7, AQ-9 and AQ-10, have similar compositions and
26   form Group C and exhibits the greatest geochemical variability in both major and trace element
27   concentrations compared with any of the pre-CI compositional groups identified at
28   Acquamorta (Fig. 4). This group of glasses (*n = 203*) is more evolved than the underlying
29   Group B glasses (See: Fig 4b-d) with higher SiO_2 (60.06 ± 0.56 wt.%) and Na_2O (7.03 ± 0.75
30   wt.%) and lower K_2O (6.93 ± 0.60 wt.%). The trace element contents of the Group C tephras
31   (*n = 43*) are characterised by higher Zr (771 ± 280 ppm), Nb (145 ± 50 ppm), Nd (95.7 ± 24.3
32   ppm), Th (70.0 ± 22.9 ppm), and significantly higher Zr/Sr ratios (116 ± 161), relative to those
33   of both Groups B and D (Fig. 4e,f).

34   The two units directly beneath the CI (AQ-12 and AQ-13) form the Group D
35   compositional group and straddle the phonolite-trachyte boundary (Fig. 4a). Group D glasses

1 ($n = 38$) show some overlap with the Group C glasses in terms of major element composition,

2 however the Group D units are more evolved having slightly higher SiO_2 (60.95 ± 0.58 wt. %)

3 and K_2O (7.40 ± 0.39 wt.%), and lower FeO_t (2.96 ± 0.23 wt.%) and Na_2O (6.28 ± 0.46 wt.%)

4 contents and can be most easily distinguished from the geochemically similar Group C

5 deposits using SiO_2 vs. K_2O plots (Fig. 4d). Levels of incompatible trace element enrichment

6 in the Group D glasses (Th = 53.6 ± 11.4 ppm, Nd = 88 ± 21 ppm and Y = 57 ± 16 ppm) are

7 restricted to those consistent with the least evolved Group C deposits (e.g. AQ-4), this

8 considerable overlap means Groups C and D glasses cannot be reliably distinguished using

9 trace element analysis alone (Fig. 4e,f).

10

6. Discussion

6.1. Composition and source of the Acquamorta tephra units

13 All samples analysed in this study can be correlated to either Campi Flegrei or Ischia based

14 on glass composition (comparing to the data of Tomlinson et al., 2012, 2014). These

15 Acquamorta analyses have also been compared to those of distal tephra layers with CVZ

16 glass compositions (Wulf et al., 2004, 2008, 2012, 2018; Bourne et al., 2010; Wutke et al.,

17 2015; Giaccio et al., 2017; McGuire et al., 2022). These new geochemical data indicate that

18 successive eruptions often share similar glass compositions (Fig. 4).

19

Ischia tephra

21 The Group A tephra deposits preserved between the MEGT and CI at Acquamorta fall within

22 the glass compositional field for Ischia deposits (Fig. 4) and are consistent with published

23 compositions for post-MEGT eruptions (Tomlinson et al., 2014). They have high SiO_2 (62.65

24 ± 0.47 wt.%) and low CaO (1.38 ± 0.13 wt.%), along with increasing K_2O and CaO and

25 decreasing Na_2O and FeO_t with increasing SiO_2 (Fig. 5a,c,d). These Acquamorta Ischia units

26 are relatively similar in thickness, do not have any particularly unique visual characteristics,

27 and are indistinguishable using both major and trace element data (Figs. 4,5); thus, they

28 cannot be correlated to other units in and around the calderas.

29 While the three Ischia units at Acquamorta fall within the broad range in glass

30 compositions characteristic of the Schiappone Tephra, their tight overlapping compositional

31 clusters make it difficult to correlate any Acquamorta unit to this particular eruption (Fig. 5c-f).

32 The TM-18-17a tephra in the LGdM sequence and the C-16 tephra from the Tyrrhenian Sea

33 have previously been correlated to the Schiappone based on complete geochemical overlap,

but with the dominant population lying within the least evolved member of the Schiappone (Tomlinson et al., 2014). Furthermore, the PRAD-1752 cryptotephra from the Adriatic Sea has also been proposed as a correlative to the Schiappone (see: Bourne et al., 2010; Tomlinson et al., 2014), but the compositions are inconsistent and, based on our acquisition of new glass chemistry , PRAD-1752 must correlate to a different unit not preserved at Acquamorta (Fig. 5c,d). Although the Acquamorta Ischia tephras show a good overlap in major element data with both the Schiappone and the equivalent TM-18-17a tephra (Fig. 5c,d), trace element data reveal all three deposits have a closer geochemical affinity with the younger TM-18-9a Ischia unit preserved in the LGdM that has a varve age of 41,420 yrs cal. BP (Fig. 5e,f), which has not been correlated to a proximal deposit on Ischia.

The three Acquamorta proximal units and the TM-18-9a tephra show overlap with the Schiappone Tephra but extend to higher Th (~9 ppm) and Nb (~1 ppm) relative to the Schiappone LGdM equivalent (TM-18-17a). The very similar compositions of these units at Acquamorta highlights that correlations to particular Ischia units both proximally and distally are problematic. Furthermore, it is not known whether these are associated with known Ischia eruptions for which there is no glass chemistry (i.e. Capo Grosso, La Roia, Chiummano; Fig. 1) or other eruptions that are not observed elsewhere. The Ischia units identified within this study re-affirm that Ischia produced multiple chemically indistinct eruptions in the 16 ka following the large MEGT eruption, and show that the magmatic system and processes prior to the eruptions were similar prior to each of these events.

Campi Flegrei tephra

The major and trace element glass compositions of tephras in Groups B, C and D are consistent with eruptions from Campi Flegrei (Fig. 4). These pre-CI Campi Flegrei groups are most clearly separated from the Ischia deposits (Group A) using SiO_2 vs. CaO, SiO_2 vs. Na_2O and Th vs. Y (Fig. 4b,c,e). These glasses display slightly decreasing FeO_t with increasing SiO_2 (Fig. 6b) and are moderately to highly evolved with Zr/Sr ratios ranging from 9.96 to 355 ppm, which is compatible with major and trace element data of other analysed pre-CI units (Tomlinson et al., 2012). The trace element data obtained for these pre-CI units does not help further distinguish the three pre-CI Campi Flegrei compositional groups, as many of the units overlap (Fig 4f-h), however some units possess distinct characteristics that may aid future individual tephra correlations.

The major element data for the nine pre-CI Campi Flegrei deposits reveal that the pre-CI deposits span a wider compositional range than previously reported for proximal pre-CI

deposits (Fig.6 a-d). The youngest group, Group D, has compositions that extend into the CI compositional field for the initial Plinian phase (Fig. 6).

It has previously been noted, using XRF whole rock data, that the pre-CI Campi Flegrei deposits have a more restricted compositional range than the CI (Pabst et al., 2008). Three pre-CI compositional groups were proposed by Pabst et al. (2008) based on whole rock and isotope data obtained from units at Trefola (Pappalardo et al., 1999). Glass compositions of a selection of these units analysed by Tomlinson et al. (2012) correspond to Pabst's Pre-CI Group 1 (TLc) and Pre-CI Group 2 (TLf). There is no glass chemistry for Pabst's Pre-CI Group 3. The Campi Flegrei chemical groups at Acquamorta do not clearly map onto those of Pabst et al. (2008), but both datasets show changes over time (Fig. 7a-c). The shifts in major and trace element glass compositions that denote the three Campi Flegrei compositional groups represent changes in the magmatic system (Fig. 4,6).

Whilst the geochemical data has enabled us to discern three compositional groups between 56 – 40 ka, the eruption units within these groups are share similar major and trace element compositions (Fig. 6). Thus, we cannot correlate individual tephra units from Acquamorta to layers in other distal or proximal records. Here we discuss the visual descriptions and detailed geochemical data of these compositional groups and discrete units, where useful, to aid future correlations.

Group B

Group B is comprised of the two lowermost tephra units: the 0.25 m thick unit of pods of clast supported pumice lapilli (AQ-2) and the 0.90 m thick deposit comprising of white/grey massive ash with a basal band of clast-supported angular pumices (AQ-3), which are separated by a well-developed paleosol (Fig.3). They present the least evolved glass compositions of the pre-CI units analysed in this study and are characterised by elevated K_2O and CaO contents relative to the other Campi Flegrei units analysed (Figs. 4d, 6d). Indeed, the alkali ratio of the glasses are elevated relative to the other Pre-CI CF glasses analysed at Acquamorta (K_2O/Na_2O = 1.36 ± 0.15). This, combined with elevated Ba and Sr contents, relative to the dominant populations of the other groups, probably indicates a lesser degree of K-feldspar fractionation.

The chrono-stratigraphically separated Group B units share partially overlapping major and trace element geochemistries of chemical compositions (Fig. 4). The glasses from the AQ-3 unit, despite slightly higher SiO_2, are less enriched than AQ-2 glasses (Fig. 4b,c). The AQ-2 unit is dominated by glasses with lower SiO_2 and higher CaO contents relative to the

overlaying AQ-3 unit and thus can be separated using the SiO_2 vs. CaO plot (Fig. 6d). The levels of incompatible trace element enrichment differ too. Whilst levels of incompatible trace element enrichment are greater in the AQ-2 glasses, which is illustrated by Nb, Zr and Th contents, they also extend to slightly lower Sr, Ba and Eu contents than those of the AQ-3 glasses, indicative of greater K-feldspar fractionation (Fig. 6e,f; Table 1).

The geochemical characteristics of the two Acquamorta Group B tephras are similar to the TLf unit at Trefola (Fig. 7), but the Al_2O_3 contents of TLf are higher suggesting that they are different eruption deposits. The trace element contents of TLf are heterogenous, encompassing the full compositional range observed in both AQ-2 and AQ-3 (Fig. 7d,e). The TLf unit has been regarded as a useful Pre-CI Campi Flegrei marker layer because of its geochemical characteristics and because it is thought to be associated with a large eruption as the deposits at Trefola is ~ 13 m thick (Orsi *et al.,* 1996; Pappalardo *et al.,* 1999; Pabst *et al.*, 2008; Tomlinson *et al.*, 2012). Our data indicate that there are at least three eruptions with the similar TLf geochemistry so correlations to TLf need to be based on more than just the chemical similarity.

Group C

The five units in Group C (AQ-4, AQ-6, AQ-7, AQ-9 and AQ-10) make up 3.50 m of the 6 m-thick exposure (Fig. 3). Group C glasses are more geochemically evolved than the underlying Group B glasses (Fig. 4a-e) and display the greatest compositional diversity of the three pre-CI Campi Flegrei groups (Fig. 7a-c). Group C deposits are characterised by lower MgO content, relative to the other two Campi Flegrei groups (Fig. 6c), and possess the highest Na_2O contents of all deposits at Acquamorta giving total alkalis values of 13.69 ± 0.46 wt.% and K_2O/Na_2O ratios of 0.99 ± 0.18. Individual units within Group C are largely indistinguishable on major element chemistry. However, the two uppermost units; AQ-9 (0.75 m thick of poorly sorted yellow ash with some laminations and accretionary lapilli) and AQ-10 (0.75 m of thick well-sorted pumices) are two of the thickest units in the sequence (See: Fig. 3) and display the greatest geochemical heterogeneity of any of the Acquamorta units (Fig. 4). Both AQ-9 and AQ-10 units plot distinctly within Group C with lower K_2O and higher Na_2O contents than the other units in this group and can easily be separated from other units which comprise the Group C glasses using SiO_2 vs. K_2O and SiO_2 vs. Na_2O plots (Fig. 4c,d). Furthermore, the AQ-9 unit has a very distinctive trace element composition representing the most enriched glasses (>70 ppm Th) at Acquamorta (Fig. 4e,f). We therefore tentatively suggest that the AQ-9 and AQ-10 units could represent a sub-group within the Group C glasses. Additionally, using the dominant population of the AQ-6 glasses, the unit can largely

be distinguished from other Group C units (AQ-4 and AQ-9) at a trace element level (Fig. 4e,f). Whilst we have been unable to correlate any of the Group C glass with proximal-distal pre-CI deposits, we propose the geochemical features of these units may aid future correlations.

The Acquamorta pre-CI Group C tephras show some geochemical similarities with the deposits from Trefola but have lower Al_2O_3 and K_2O, and elevated Na_2O contents (Fig 7a-c). The 2 cm thick TF-6 tephra in the Fucino record (130 km north of Campi Flegrei; Fig. 2b) has been correlated to TLc (Giaccio et al., 2017). However, the TF-6 unit has much lower Al_2O_3 content (~1.25 wt%) than the TLc tephra unit (Fig.7c), and is more similar to Acquamorta Group C glasses. The TF-6 unit is compositionally identical to the AQ-4 unit, which has distinctive Na_2O contents relative to the rest of the Group C glasses (Fig. 7b). We argue that the TF-6 unit is not the distal equivalent of the TLc but instead most likely correlates to AQ-4. As there is no published trace element data the TF-6 unit we are unable to verify the correlation. While major element concentrations in AQ-4 are fairly homogenous, this >0.5 m thick unit has a somewhat bimodal trace element signature (e.g. two Th populations at 50 and 55 ppm; Figs. 4e,f, 6e,f), which could prove useful for future correlation purposes.

Group D

The two eruption units identified directly below the CI (AQ-12 and AQ-13) at Acquamorta are compositionally distinct relative to other pre-CI groups with a Campi Flegrei chemistry. Both units are 2 cm thick fine ash deposits and are separated by a well-developed paleosol (Fig. 3). Group D glasses have higher SiO_2 (60.95 ± 0.58 wt.%) and K_2O (7.40 ± 0.39 wt.%) and slightly lower Na_2O (6.28 ± 0.465 wt.%) than the underlying pre-CI Group C Campi Flegrei deposits (Table 1; Fig. 4c,d). The only tephra deposit from the Group D glasses with trace element data (AQ-13) displays significant heterogeneity and consequently overlaps with many of the pre-CI tephras from both Group B and Group C (Fig. 4e,f). However, on the Nb vs. Th plot it is clear that at overlapping Th content the dominant population of AQ-13 (ca. 53 ppm Th) contains lower levels of Nb enrichment relative to the other pre-CI tephra units (e.g., AQ-4), and is instead more consistent with the overlying CI deposits. Both the AQ-12 and AQ-13 identified at Acquamorta are the only units at the site to overlap with the CI in both major and trace elements (Fig. 6) and therefore justifies their classification as a separate compositional group (Group D).

These Group D glasses are compositionally similar to the initial fallout phase of the CI eruption (Fig. 8). Major and trace element data show considerable overlap of the Group D glasses with the four distal LGdM TM-18-1a-d visible tephra units (Fig. 8) erupted c. 600 years before the CI whose geochemical affinity with the CI deposit has previously been reported

1 (see: Wutke et al., 2015). The TM-18-1d tephra deposit is geochemically distinct relative to

2 the three younger TM-18-1a-c tephra deposits (see: Wutke et al., 2015). The AQ-12 and AQ-

3 13 tephra units (which comprise the Group D glasses) display a greater geochemical similarity

4 with the TM-18-1a-c tephra deposits (Fig. 8c-f). Due to the inability to geochemically

5 distinguish the two units which from the Group D compositional group or the three TM-18-1a-

6 c tephras, we are unable to more precisely resolve this proximal-distal correlation. It is

7 important to note that whilst we cannot provide a unit-to-unit correlation, we suggest a

8 geochemical package-to-package correlation between the Group D and TM-18-1a-c units.

9 Other distal records located in northeast Greece, Ioannina (McGuire et al., 2002) and

10 Tenaghi Philippon (Wulf et al., 2018), have reported a total of eight cryptotephras beneath the

11 CI with overlapping major element geochemical compositions to the CI (Figs. 1b, 8a,b). Five

12 of these cryptotephra deposits are believed to be reworked CI deposits (Wulf et al., 2018;

13 McGuire et al., 2022). Wulf et al., (2018) has tentatively correlated one other cryptotephra

14 deposit from Tenaghi Philippon (TP05-13.34) with the LGdM TM-18-1d tephra deposit due to

15 major and trace element similarities. However, we observe that the composition of the TP05-

16 13.34 glasses have higher K_2O and SiO_2 contents than the TM-18-1d glasses, and thus do

17 not correlate. TP05-13.34 is compositionally similar to the younger TM-18-1-a-c tephra

18 deposits, the I08-30.74 and 108-31.17 cryptotephra deposits preserved in Ioannina, and the

19 AQ-12 and AQ-13 tephra deposits at Acquamorta (Fig. 8). Due to the compositional similarity

20 both within the Acquamorta Group D glasses and glasses preserved just below the CI in distal

21 sites, it has not been possible to correlate particular units. These two Group D Acquamorta

22 units are the first proximal deposits identified that are compositionally similar to the CI. These

23 could possibly correlate to distal tephra units in Italy (LGdM; Wutke et al., 2015) and Greece

24 (Tenaghi Philippon: Wulf et al., 2018; Ioannina: McGuire et al., 2022) or could be separate

25 small eruptions prior to the CI. Ultimately the identification of the first proximal units displaying

26 the same compositions as the TM-18-1a-c tephras that were erupted less than 600 years

27 before the CI highlights that there were eruptions with similar glass compositions before the

28 CI, and that records that assigned layers beneath the CI as reworked layers based on the

29 chemistry may need to be revisisted (e.g. McGuire et al., 2022).

30

31 **6.2. Eruption history**

32 The Acquamorta outcrop is a unique record on the western sector of the CI caldera. The site

33 records twelve eruption deposits between the MEGT (56 ka) and the CI (40 ka) eruptions;

34 three from Ischia and nine from Campi Flegrei. We have not been able to correlate to tephra

35 units elsewhere so we are unable to use these deposits to constrain size or dispersal of the

1　eruptions. The Acquamorta units are thin (Fig. 3), which is consistent with prevailing winds
2　that indicate the position is unlikely to have been on the dispersal axis. Most mapped eruption
3　dispersals extend towards the east with little or nothing preserved at Acquamorta (Rosi et al.,
4　1999; Costa et al., 2008). Based on what is known the size and the dispersal of other Campi
5　Flegrei eruptions (e.g., D'Antonio et al., 1999; Smith et al., 2011), these tephra layers likely
6　represent eruptions with volumes of ≥1 km^3 DRE and a Magnitude of ≥5.

7　This study provides evidence for the tempo of volcanism of these two caldera systems both in
8　the lead up to, and in the aftermath of caldera generating eruptions and thus has hazard
9　assessment implications for these closely spaced, highly active volcanic centres. Ultimately,
10　these findings highlight the need for integration of records from the proximal through to distal
11　settings in order to generate the most complete eruption histories possible (see Figs. 1,2).

12

13　***Ischia***

14　The three Ischia units that outcrop at Acquamorta highlight difficulties in in terms of chemically
15　correlating and distinguishing eruption units, and thus obtaining a detailed record of the post-
16　MEGT Ischia eruption frequency . Whilst the eruption stratigraphy of Ischia is better preserved
17　in proximal locations than that of Campi Flegrei (e.g. Poli et al., 1987; Brown et al., 2008,
18　2014) and many of the Ischia units have been geochemically characterised (see: Tomlinson
19　et al., 2014), we have been unable to correlate any of the post-MEGT Ischia units preserved
20　at Acquamorta to a particular eruption deposit because the glass compositions of the tephra
21　units are too similar. It is likely that the proximal deposits on Ischia, mostly outcropping in cliffs
22　and coastal sections, represent a substantially incomplete record, lacking units that are in
23　distal records. The Acquamorta Ischia units show overlap with the Schiappone on major and
24　trace element compositions, but do not display the full compositional range observed in the
25　Schiappone unit sampled on Ischia (Tomlinson et al., 2014). The tight compositional group
26　(Fig. 5c-f) may be due to changes in wind direction during the eruption and only part of the
27　eruption deposit is preserved at Acquamorta. Nevertheless, all three Ischia units at
28　Acquamorta show a greater degree of geochemical similarity to the TM-18-9a deposit
29　preserved 130 km east in LGdM, which has an age of 41.42 ka varve yrs BP (Fig. 5c-f). The
30　TM-18-9a is stratigraphically positioned above the distal equivalent of the MEGT (TM-19) and
31　has not been correlated to a proximal equivalent (Tomlinson et al., 2014) and due to the
32　homogenous compositions of the three units at Acquamorta, we are unable to identify which,
33　if any, of these tephras is the proximal equivalent of this distal layer. The identification of these
34　three proximal units with repeated chemical signatures suggests that it is not possible to
35　correlate to a particular Ischia tephra within this time interval, unless they have the wider

compositional range of Schiappone, or are slightly distinct like the deposits from Agnone or Pietre Rosse eruptions.

Distal tephra deposits have been correlated to the Schiappone eruption using major element glass chemistry data. However, given the new proximal data generated by this study and the geochemical affinity with LGdM tephras, we argue that previous correlations to the Schiappone need to be revisited, such as the PRAD-1752 cryptotephra preserved ~8 cm below the CI in the Adriatic Sea (Bourne et al., 2010) and to other Ischia deposits across the Mediterranean including the 20 cm thick SMP1-a tephra deposit preserved beneath the CI on the Sorrento Peninsula with the TM-18-1 cryptotephra deposit located 50km east (Wutke et al., 2015). The lack of detailed geochemical characterisation of previously identified proximal post-MEGT Ischia units (i.e. Chiummano, La Roia and Capo Grosso) may result in miscorrelations, as has been argued for more widespread Ischia deposits (D'Antonio et al., 2021). This study presents geochemical data for Ischia deposits that have previously been unreported which may relate to the Ischia eruption record being incomplete or the lack of chemical data for some Ischia units described and mentioned above.

Campi Flegrei

The data presented in this study is a significant addition to the eruption history of the highly active Campi Flegrei caldera volcano. The identification of the nine Pre-CI Campi Flegrei tephra deposits between MEGT and CI marker units provides new insight into activity in the lead up to the CI super-eruption; a time-interval where a comprehensive long-term eruption history has been lacking (see: Fig. 1). It is not possible to discern each of the deposits on the basis of geochemical data alone as many successive deposits have overlapping and repeating geochemistries. However, two compositional shifts are observed over time, denoting packages of units. These packages can be correlated over distance and provide some insight into the magmatic system feeding this extremely productive phase of the volcano.

This study pulls together evidence in the proximal and distal tephra record and demonstrates that there was heightened activity prior to the CI caldera forming event, which has implications for hazard evaluation (Pappalardo et al., 1999; Di Vivo et al., 2001; Di Vito et al., 2008; Wulf et al., 2004; Tomlinson et al., 2012; Wutke et al., 2015; Giaccio et al., 2017; Manella et al., 2019). Further detailed stratigraphic and geochemical characterisation of proximal outcrops below the CI caldera is required to generate a more complete eruption history and refine hazard assessments for Campi Flegrei. Furthermore, this can be used to further constrain the magmatic processes preceding very large, caldera-forming eruptions.

6.3. Magmatic system

The compositional data presented here provides further insight into the magmatic systems beneath both Ischia and Campi Flegrei between 56 and 40 ka. The glass compositions of the deposits are evolved and largely homogenous suggesting that each eruption tapped a single magma batch. This is consistent with these Acquamorta deposits between the MEGT and CI being associated with relatively small eruptions (Magnitude ≤5) as the large events from both Campi Flegrei and Ischia tend to tap multiple, homogeneous magma batches, such as the Campanian Ignimbrite (e.g. Smith et al., 2016) and Masseria de Monte (Albert et al., 2019) from Campi Flegrei, and the Schiappone and MEGT from Ischia (Tomlinson et al., 2014).

The three post-MEGT Ischia units preserved at Acquamorta provide limited insight into the magmatic system beneath Ischia as there are at least six eruption deposits from Ischia in this time period (Fig. 1). Whole-rock and isotopic data from Brown et al. (2014) shows a shift after the MEGT with the influx of less evolved and isotopically distinct melt. The Capo Grosso, La Roia and Chiummano eruptions that followed the MEGT and preceded the Schiappone (Fig. 1,5c-f) are distinct from each other and less evolved than the Schiappone, but the similar isotopic compositions indicate that they may have the same melt with each eruption tapping it at different stages of its evolution. The Schiappone tephra is compositionally heterogeneous tapping multiple magma batches (Tomlinson et al., 2014), and one of the melt compositions is the same as that tapped by the three Ischia eruptions that are preserved at Acquamorta. It is not clear whether these deposits precede, succeed, or include the Schiappone. In any case, since the major and trace element compositions are identical for these three Ischia eruptions it shows that the melt in the system did not evolve much between the eruptions.

Previous studies that investigated the Campi Flegrei magmatic system pre-CI focussed on whole-rock and limited isotopic data from a few of the deposits (Pappalardo et al., 1999, Pappalardo et al., 2002; Pabst et al., 2008) and did not provide a detailed insight into the system. Our new data shows that similar melt compositions are commonly erupted by successive events, and there were a couple of compositional shifts over time; between Group B and C, and Group C and D.

The two units in Group B share similar major elements and trace element compositions. The compositional change that occurs between Group B and C is an increase in Na_2O, Rb, Y, Zr, Nb, REE, Th, and U, and a decrease in K_2O, CaO, V, and Sr (Fig. 4, 6; Table 1). While the four units in Group C share similar major element compositions and the trace element compositions are homogeneous, the trace element compositions change through the sequence. The compositions of each unit extend to lower V concentrations, and

higher Rb, Y, Zr, Nb, REE, Ta, Th concentrations than the previous unit (Table 1). These temporal changes are consistent with crystallisation and evolution of the melt, and the lack of changes in the major elements suggesting that the amount of crystallisation was limited. The shift between Group C and D is marked by a subtle change in major elements to slightly higher SiO_2 and lower Na_2O contents (Fig. 4). While the trace element ranges observed by Group C and D overlap, and the shift between the groups is marked by a return to concentrations that are observed at the start of Group B, i.e. melts with lower Rb, Y, Zr, Nb, REE, Ta, and Th concentrations. The two Acquamorta units in Group D are compositionally identical to each other and the melt that was tapped in the Plinian phase of the CI (Tomlinson et al., 2012; Smith et al., 2016) that overlies them. At least four eruptions occurred in Group D as four units directly below the CI in the LGdM record (TM-18-1a-d) have major and trace element compositions that are identical to Group D composition (Wutke et al., 2015; Fig. 8a-f). Data from one of the pre-CI units in Pabst et al. (2008) indicates that at least one of the eruptions before the CI has similar isotope compositions, which suggests that the large homogeneous melt body that fed the first phases of the CI eruption was at least partly in place before the Group D eruptions. These pre-CI Group D eruptions would have only tapped relatively small portions of the melt, and the identical major and trace element compositions indicate there was little evolution of this melt between these Group D and the CI. Given that the Group D and CI compositions are different to those erupted earlier (Group B and C) it implies that the CI magma that fed the Plinian phase and portions of the PDCs (>150 km^3 DRE; Marti et al., 2016) did not exclusively occupy the upper crust beneath Campi Flegrei in the 14 ka prior to the CI eruption. In fact, the high-resolution chronology from the LGdM record suggests that the distally dispersed Group D eruptions occurred within 600 years of the CI (Wutke et al., 2015).

Both Ischia and Campi Flegrei tap compositionally similar melts over time, which implies that some of the eruptions are only tapping portions of the homogenous system that it is not evolving much over time. Although we do not have a precise chronology of the pre-CI events, the fact that there are well developed paleosols between the deposits implies that the systems were similar over thousands of years. Similar patterns with successive eruptions tapping compositionally similar melts is observed at other times at Campi Flegrei, such as prior to and following the NYT eruption (Albert et al., 2019; Forni et al., 2018; Smith et al., 2011). The main compositional shifts observed over time (i.e. between Group B and C, and Group C and D) likely reflect the new input of melt into the upper crust beneath Campi Flegrei, and likely match the isotopic shifts that observed by Pabst et al. (2008) in the pre-CI deposits.

7. Conclusion

New major and trace element glass data for twelve tephra deposits preserved between the MEGT and CI within the Acquamorta outcrop located on the western side of the CI caldera wall have been acquired and are presented. We have been able to correlate all twelve deposits to a volcanic source within the CVZ; three units are from Ischia eruptions and nine units are from Campi Flegrei eruptions. The compositional data obtained indicates that successive eruptions from each volcano are broadly compositionally homogenous, with small compositional shifts over time.

The three Ischia tephra deposits are compositionally indistinguishable at both the major and trace element level and have not been correlated to any proximal or distal tephra units. These are compositionally similar to the most evolved component of the Schiappone tephra, the largest post-MEGT Ischia eruption, with none showing the full compositional range that is diagnostic of this particular eruption deposit. Whilst we cannot rule out that one of these tephra deposits at Acquamorta may represent the Schiappone, there are another two other eruptions with a similar geochemical composition. Ultimately the identification of these geochemically indistinguishable units suggests that the post-MEGT eruption history for Ischia is not well resolved and may be incomplete, and care must be taken when correlating post-MEGT Ischia units.

We have shown that the nine pre-CI Campi Flegrei units from Acquamorta form three distinct geochemical clusters and demonstrate the ability to discern temporal differences in glass chemistry of the volcano through time. These data indicate the pre-CI Campi Flegrei eruptions were fed by highly, but differently, evolved magmas, similar to the post-NYT Campi Flegrei deposits (Smith et al., 2011). These groups follow a general trend of becoming increasingly evolved in the lead-up to the CI, with the youngest units (Group D) very similar in composition to the magma erupted during the Plinian phase of the CI eruption (Fig.8). Whilst trace data was obtained for several units, they are not as useful as the major elements for discriminating the three pre-CI Campi Flegrei compositional groups (Fig. 4a-h). The most useful elements for distinguishing the pre-CI Campi Flegrei deposits are Al_2O_3, CaO, Na_2O, K_2O, Nb and Th. We have identified multiple tephra deposits at Acquamorta with the same chemistry as both known proximal (Group B with the TLf tephra; Tomlinson et al., 2012) and distal (Group D with the TM-18-1a-c units; Wutke et al., 2015) tephra deposits. Thus, these correlations are not to particular eruptions and instead correlations can only be made to a package of units with similar chemistry (i.e. the Group), which erupted over the order of several thousand years.

1   The findings from this study highlight the need for further detailed chrono-stratigraphic

2   and geochemical data from tephra deposits located across the CI caldera to generate more

3   complete eruption histories and magmatic systems for the volcanoes that form the CVZ and

4   thus improve the hazard assessments for some of Europe's most active volcanoes. Only once

5   this has been undertaken will it be possible to establish combine proximal and distal records

6   to establish a detailed tephrostratigraphy and establish which are the likely eruptions that

7   resulted in tephra dispersal across the southern Mediterranean region.

8

17

References

19 Albert, P.G., Hardiman, M., Keller, J., Tomlinson, E.L., Smith, V.C., Bourne, A.J., Wulf, S.,
20   Zanchetta, G., Sulpizio, R., Müller, U.C., Pross, J., Ottolini, L., Matthews, I.P., Blockley, S.P.E.
21   & Menzies, M.A. (2015) 'Revisiting the Y-3 tephrostratigraphic marker: A new diagnostic glass
22   geochemistry, age estimate, and details on its climatostratigraphical context'. Quaternary
23   Science Reviews 118 p.pp. 105–121.

24 Albert, P.G., Giaccio, B., Isaia, R., Costa, A., Niespolo, E.M., Nomade, S., Pereira, A., Renne, P.R.,
25   Hinchliffe, A., Mark, D.F., Brown, R.J. & Smith, V.C. (2019) 'Evidence for a large-magnitude
26   eruption from Campi Flegrei caldera (Italy) at 29 ka', Geology, 47(7), pp. 595–599.

27 Alessio, M., Bella, F., Improta, S., Belluomini, G., Calderoni, G., Cortesi, C. & Turi, B. (1976)
28   'University of Rome carbon-14 dates XIV', Radiocarbon, 18(3), pp.321-349.

29 Bourne, A.J., Lowe, J.J., Trincardi, F., Asioli, A., Blockley, S.P.E., Wulf, S., Matthews, I.P., Piva, A.
30   & Vigliotti, L. (2010) 'Distal tephra record for the last ca 105,000 years from core PRAD 1-2 in
31   the central Adriatic Sea: implications for marine tephrostratigraphy', Quaternary Science
32   Reviews, 29(23–24), pp. 3079–3094.

33 Bronk Ramsey, C., Albert, P.G., Blockley, S.P.E., Hardiman, M., Housley, R.A., Lane, C.S., Lee,
34   S., Matthews, I.P., Smith, V.C. & Lowe, J.J. (2015) 'Improved age estimates for key Late
35   Quaternary European tephra horizons in the RESET lattice', Quaternary Science Reviews,
36   118pp. 18–32.

Brown, R.J., Orsi, G. & de Vita, S. (2008) 'New insights into Late Pleistocene explosive volcanic activity and caldera formation on Ischia (southern Italy)', Bulletin of Volcanology 2007 70:5, 70(5), pp. 583–603.

Brown, R.J., Civetta, L., Arienzo, I., Moretti, R., Orsi, G., Tomlinson, E.L., Albert, P.G. & Menzies, M.A. (2014) 'Geochemical and isotopic insights into the assembly, evolution and disruption of a magmatic plumbing system before and after a cataclysmic caldera-collapse eruption at Ischia volcano (Italy)', Contrib Mineral Petrol, 168p. 1035.

Buchner, G., Italiano, A. & Vita-Finzi, C. (1996) 'Recent uplift of Ischia, southern Italy',Geological Society, London, Special Publications. 110 (1), 249–252.

Costa, A., Dell'Erba, F., Vito, M.A., Isaia, R., Macedonio, G., Orsi, G. & Pfeiffer, T. (2008) 'Tephra fallout hazard assessment at the Campi Flegrei caldera (Italy)' Bulletin of Volcanology 71, 259–273.

Cioni, R., Santacroce, R. & Sbrana, A. (1999) 'Pyroclastic deposits as a guide for reconstructing the multi-stage evolution of the Somma-Vesuvius Caldera', Bulletin of Volcanology, 61(4), pp. 207–222.

Civetta, L., Galati, R. & Santacroce, R. (1991) 'Magma mixing and convective compositional layering within the Vesuvius magma chamber', Bulletin of Volcanology 1991 53:4, 53(4), pp. 287–300.

D'Antonio, M., Civetta, L., Orsi, G., Pappalardo, L., Piochi, M., Carandente, A., Vita, S.D., Vito, M.A.D. & Isaia, R. (1999). 'The present state of the magmatic system of the Campi Flegrei caldera based on a reconstruction of its behavior in the past 12 ka', Journal of Volcanology and Geothermal Research 91, 247–268.

D'Antonio, M., Arienzo, I., Brown, R.J., Petrosino, P., Pelullo, C. & Giaccio, B. (2021) 'Petrography and mineral chemistry of monte epomeo green tuff, ischia island, south italy: Constraints for identification of the y-7 tephrostratigraphic marker in distal sequences of the central mediterranean', Minerals, 11(9), p. 955.

De Astis, G., Pappalardo, L. & Piochi, M. (2004) 'Procida volcanic history: New insights into the evolution of the Phlegraean Volcanic District (Campania region, Italy)', Bulletin of Volcanology, 66(7), pp. 622–641.

Donato, P., Albert, P.G., Crocitti, M., De Rosa, R. & Menzies, M.A. (2016) 'Tephra layers along the southern Tyrrhenian coast of Italy: Links to the X-5 & X-6 using volcanic glass geochemistry', Journal of Volcanology and Geothermal Research, 317pp. 30–41.

Fedele, F., Giaccio, B., Isaia, R. & Orsi, G. (2003) 'The Campanian Ignimbrite Eruption, Heinrich Event 4, and Palaeolithic Change in Europe: a High-Resolution Investigation', Geophysical Monograph Series, 139pp. 301–325.

Forni, F., Degruyter, W., Bachmann, O., De Astis, G. & Mollo, S. (2018) 'Long-Term magmatic evolution reveals the beginning of a new caldera cycle at Campi Flegrei', Science Advances, 4(11).

Giaccio, B., Nomade, S., Wulf, S., Isaia, R., Sottili, G., Cavuoto, G., Galli, P., Messina, P., Sposato, A., Sulpizio, R. & Zanchetta, G. (2012) 'The late MIS 5 Mediterranean tephra markers: a reappraisal from peninsular Italy terrestrial records', Quaternary Science Reviews, 56pp. 31–45.

Giaccio, B., Niespolo, E.M., Pereira, A., Nomade, S., Renne, P.R., Albert, P.G., Arienzo, I., Regattieri, E., Wagner, B., Zanchetta, G., Gaeta, M., Galli, P., Mannella, G., Peronace, E.,

1   Sottili, G., Florindo, F., Leicher, N., Marra, F. & Tomlinson, E.L. (2017) 'First integrated
2   tephrochronological record for the last ~190 kyr from the Fucino Quaternary lacustrine
3   succession, central Italy', Quaternary Science Reviews, 158pp. 211–234.

4   Isaia, R., Marianelli, P. & Sbrana, A. (2009) 'Caldera unrest prior to intense volcanism in Campi
5   Flegrei (Italy) at 4.0 ka B.P.: Implications for caldera dynamics and future eruptive scenarios',
6   Geophysical Research Letters, 36(21).

7   Isaia, R., Vitale, S., Marturano, A., Aiello, G., Barra, D., Ciarcia, S., Iannuzzi, E. & Tramparulo,
8   F.D.A. (2019) 'High-resolution geological investigations to reconstruct the long-term ground
9   movements in the last 15 kyr at Campi Flegrei caldera (southern Italy)', Journal of Volcanology
10   and Geothermal Research, 385, pp.143-158.

11   Jochum, K.P., Stoll, B., Herwig, K., Willbold, M., Hofmiann, A.W., Amini, M., Aarburg, S.,
12   Abouchami, W., Hellebrand, E., Mocek, B., Raczek, I., Stracke, A., Alard, O., Bouman, C.,
13   Becker, S., Dücking, M., Brätz, H., Klemd, R. & De Bruin, D. (2006) 'MPI-DING reference
14   glasses for in situ microanalysis: New reference values for element concentrations and isotope
15   ratios', Geochemistry, Geophysics, Geosystems, 7(2).

16   Keller, J., Ryan, W.B.F., Ninkovich, D. & Altherr, R. (1978) 'Explosive volcanic activity in the
17   Mediterranean over the past 200,000 yr as recorded in deep-sea sediments), Geological
18   Society of America Bulletin, 89(4), pp.591-604.

19   Marti, A., Folch, A., Costa, A., & Engwell, S. (2016) 'Reconstructing the plinian and co-ignimbrite
20   sources of large volcanic eruptions: A novel approach for the Campanian Ignimbrite.' Scientific
21   Reports, 1–11.

22   McGuire, A.M., Lane, C.S., Roucoux, K.H., Albert, P.G. & Kearney, R. (2022) 'The dating and
23   correlation of an eastern Mediterranean lake sediment sequence: a 46 – 4 ka
24   tephrostratigraphy for Ioannina (NW Greece)', Journal of Quaternary Science, 37(8), pp.1313-
25   1331.

26   Monaco, L., Palladino, D.M., Albert, P.G., Arienzo, I., Conticelli, S., Di Vito, M., Fabbrizio, A.,
27   D'Antonio, M., Isaia, R., Manning, C.J., Nomade, S., Pereira, A., Petrosino, P., Sottili, G.,
28   Sulpizio, R., Zanchetta, G. & Giaccio, B. (2022) 'Linking the Mediterranean MIS 5 tephra
29   markers to Campi Flegrei (southern Italy) 109–92 ka explosive activity and refining the
30   chronology of MIS 5c-d millennial-scale climate variability', Global and Planetary Change,
31   211p. 103785.

32   Munno, R. & Petrosino, P. (2007) 'The late Quaternary tephrostratigraphical record of the San
33   Gregorio Magno basin (southern Italy)', Journal of Quaternary Science, 22(3), pp. 247–266.

34   Newhall, C.G. & Self, S. (1982) 'The volcanic explosivity index (VEI) an estimate of explosive
35   magnitude for historical volcanism', Journal of Geophysical Research: Oceans, 87(C2), pp.
36   1231–1238.

37   Orsi, G., Gallo, G. & Zanchi, A. (1991) 'Simple-shearing block resurgence in caldera depressions.
38   A model from Pantelleria and Ischia', Journal of Volcanology and Geothermal Research, 47(1–
39   2), pp. 1–11.

40   Orsi, G., De Vita, S. & Di Vito, M. (1996) 'The restless, resurgent Campi Flegrei nested caldera
41   (Italy): constraints on its evolution and configuration', Journal of Volcanology and Geothermal
42   Research, 74(3–4), pp. 179–214.

43   Orsi, G., Di Vito, M.A. & Isaia, R. (2004) 'Volcanic hazard assessment at the restless Campi Flegrei
44   caldera', Bulletin of Volcanology 2004 66:6, 66(6), pp. 514–530.

Pabst, S., Wörner, G., Civetta, L. & Tesoro, R. (2008) Magma chamber evolution prior to the Campanian Ignimbrite and Neapolitan Yellow Tuff eruptions (Campi Flegrei, Italy),

Pappalardo, L., Civetta, L., D'Antonio, M., Deino, A., Di Vito, M., Orsi, G., Carandente, A., De Vita, S., Isaia, R. & Piochi, M. (1999) 'Chemical and Sr-isotopical evolution of the Phlegraean magmatic system before the Campanian Ignimbrite and the Neapolitan Yellow Tuff eruptions', Journal of Volcanology and Geothermal Research, 91(2–4), pp. 141–166.

Paterne, M., Guichard, F., Labeyrie, J., Gillot, P.Y. & Duplessy, J.C. (1986) 'Tyrrhenian Sea tephrochronology of the oxygen isotope record for the past 60,000 years', Marine Geology, 72(3–4), pp. 259–285.

Paterne, M., Guichard, F. & Labeyrie, J. (1988) 'Explosive activity of the South Italian volcanoes during the past 80,000 years as determined by marine tephrochronology', Journal of Volcanology and Geothermal Research, 34(3–4), pp. 153–172.

Perrotta, A. & Scarpati, C. (1994) 'The dynamics of the Breccia Museo eruption (Campi Flegrei, Italy) and the significance of spatter clasts associated with lithic breccias' Journal of Volcanology and Geothermal Research, 59(4), pp.335-355.

Perrotta, A., Scarpati, C., Luongo, G. & Morra, V. (2010) 'Stratigraphy and volcanological evolution of the southwestern sector of Campi Flegrei and Procida Island, Italy', Stratigraphy and geology of volcanic areas, pp.171-91.

Poli, S., Chiesa, S., Gillot, P.Y., Gregnanin, A. & Guichard, F. (1987) 'Chemistry vs. time in the volcanic complex of Ischia (Gulf of Naples, Italy): evidence of successive magmatic cycles', Contributions to Mineralogy and Petrology, 95(3), pp. 322–335.

Di Renzo, V., Arienzo, I., Civetta, L., D'Antonio, M., Tonarini, S., Di Vito, M.A. & Orsi, G. (2011) 'The magmatic feeding system of the Campi Flegrei caldera: Architecture and temporal evolution', Chemical Geology, 281(3–4), pp. 227–241.

Rolandi, G., Bellucci, F., Heizler, M.T., Belkin, H.E. & De Vivo, B. (2003) 'Tectonic controls on the genesis of ignimbrites from the Campanian Volcanic Zone, southern Italy', Mineralogy and Petrology 2003 79:1, 79(1), pp. 3–31.

Rosi, M., Sbrana, A. & Vezzoli, L. (1988) 'Correlazioni tefrostratigraphiche di alcuni livelli di Ischia, Procida e Campi Flegrei', Memorie della Societa Geologica Italiana, 41pp. 1015–1027.

Rosi, M., Vezzoli, L., Castelmenzano, A. & Grieco, G. (1999) Plinian pumice fall deposit of the Campanian Ignimbrite eruption (Phlegraean Fields, Italy). Journal of Volcanology and Geothermal Research, 91, 179–198.

Santacroce, R., Cristofolini, R., La Volpe, L., Orsi, G. & Rosi, M. (2003) 'Italian active volcanoes', Episodes Journal of International Geoscience, 26(3), pp. 227–234.

Scandone, R., Bellucci, F., Lirer, L. & Rolandi, G. (1991) 'The structure of the Campanian Plain and the activity of the Neapolitan volcanoes (Italy)', Journal of Volcanology and Geothermal Research, 48(1–2), pp. 1–31.

Shane, P., Nairn, I.A., Martin, S.B. & Smith, V.C. (2008) 'Compositional heterogeneity in tephra deposits resulting from the eruption of multiple magma bodies: implications for tephrochronology', Quaternary International, 178(1), pp. 44–53.

Smith, V.C., Isaia, R. & Pearce, N.J.G. (2011) 'Tephrostratigraphy and glass compositions of post-15 kyr Campi Flegrei eruptions: Implications for eruption history and chronostratigraphic markers', Quaternary Science Reviews, 30(25–26), pp. 3638–3660.

Smith, V.C., Isaia, R., Engwell, S.L. & Albert, P.G. (2016) 'Tephra dispersal during the Campanian Ignimbrite (Italy) eruption: implications for ultra-distal ash transport during the large caldera-forming eruption', Bulletin of Volcanology 78.

Sulpizio, R., Zanchetta, G., D'Orazio, M., Vogel, H. & Wagner, B. (2010) 'Tephrostratigraphy and tephrochronology of lakes Ohrid and Prespa, Balkans', Biogeosciences, 7(10), pp. 3273–3288.

Tomlinson, E.L., Thordarson, T., Müller, W., Thirlwall, M. & Menzies, M.A. (2010) 'Microanalysis of tephra by LA-ICP-MS — Strategies, advantages and limitations assessed using the Thorsmörk ignimbrite (Southern Iceland)', Chemical Geology, 279(3–4), pp. 73–89.

Tomlinson, E.L., Arienzo, I., Civetta, L., Wulf, S., Smith, V.C., Hardiman, M., Lane, C.S., Carandente, A., Orsi, G., Rosi, M., Müller, W. & Menzies, M.A. (2012) 'Geochemistry of the Phlegraean Fields (Italy) proximal sources for major Mediterranean tephras: Implications for the dispersal of Plinian and co-ignimbritic components of explosive eruptions', Geochimica et Cosmochimica Acta, 93pp. 102–128.

Tomlinson, E.L., Albert, P.G., Wulf, S., Brown, R.J., Smith, V.C., Keller, J., Orsi, G., Bourne, A.J. & Menzies, M.A. (2014) 'Age and geochemistry of tephra layers from Ischia, Italy: Constraints from proximal-distal correlations with Lago Grande di Monticchio', Journal of Volcanology and Geothermal Research, 287pp. 22–39.

Tomlinson, E.L., Smith, V.C., Albert, P.G., Aydar, E., Civetta, L., Cioni, R., Çubukçu, E., Gertisser, R., Isaia, R. & Menzies, M.A. (2015) 'The major and trace element glass compositions of the productive Mediterranean volcanic sources: tools for correlating distal tephra layers in and around Europe', Quaternary Science Reviews, 118pp. 48–66.

Vezzoli, L. ed., 1988. *Island of Ischia*. Consiglio nazionale delle ricerche.

Vitale, S. & Isaia, R. (2014) 'Fractures and faults in volcanic rocks (Campi Flegrei, southern Italy): insight into volcano-tectonic processes', International Journal of Earth Sciences, 103, pp. 801-819.

Di Vito, M.A., Isaia, R., Orsi, G., Southon, J., De Vita, S., D'Antonio, M., Pappalardo, L. & Piochi, M. (1999) 'Volcanism and deformation since 12,000 years at the Campi Flegrei caldera (Italy)', Journal of Volcanology and Geothermal Research, 91(2–4), pp. 221–246.

Di Vito, M.A., Sulpizio, R., Zanchetta, G. & D'Orazio, M. (2008) 'The late Pleistocene pyroclastic deposits of the Campanian Plain: New insights into the explosive activity of Neapolitan volcanoes', Journal of Volcanology and Geothermal Research, 177(1), pp. 19–48.

De Vivo, B., Rolandi, G., Gans, P.B., Calvert, A., Bohrson, W.A., Spera, F.J. & Belkin, H.E. (2001) 'New constraints on the pyroclastic eruptive history of the Campanian volcanic Plain (Italy)', Mineralogy and Petrology 2001 73:1, 73(1), pp. 47–65.

Wulf, S., Kraml, M., Brauer, A., Keller, J. & Negendank, J.F.W. (2004) 'Tephrochronology of the 100 ka lacustrine sediment record of Lago Grande di Monticchio (southern Italy)', Quaternary International, 122(1), pp. 7–30.

1   Wulf, S., Kraml, M. & Keller, J. (2008) 'Towards a detailed distal tephrostratigraphy in the Central
2   Mediterranean: The last 20,000 yrs record of Lago Grande di Monticchio', Journal of
3   Volcanology and Geothermal Research, 177(1), pp. 118–132.

4   Wulf, S., Keller, J., Paterne, M., Mingram, J., Lauterbach, S., Opitz, S., Sottili, G., Giaccio, B.,
5   Albert, P.G., Satow, C., Tomlinson, E.L., Viccaro, M. & Brauer, A. (2012) 'The 100-133 ka
6   record of Italian explosive volcanism and revised tephrochronology of Lago Grande di
7   Monticchio', Quaternary Science Reviews, 58pp. 104–123.

8   Wulf, S., Hardiman, M.J., Staff, R.A., Koutsodendris, A., Appelt, O., Blockley, S.P.E., Lowe, J.J.,
9   Manning, C.J., Ottolini, L., Schmitt, A.K., Smith, V.C., Tomlinson, E.L., Vakhrameeva, P.,
10   Knipping, M., Kotthoff, U., Milner, A.M., Müller, U.C., Christanis, K. & Kalaitzidis, S.(2018) 'The
11   marine isotope stage 1–5 cryptotephra record of Tenaghi Philippon, Greece: Towards a
12   detailed tephrostratigraphic framework for the Eastern Mediterranean region', Quaternary
13   Science Reviews, 186pp. 236–262.

14   Wutke, K., Wulf, S., Tomlinson, E.L., Hardiman, M., Dulski, P., Luterbacher, J. & Brauer, A. (2015)
15   'Geochemical properties and environmental impacts of seven Campanian tephra layers
16   deposited between 40 and 38 ka BP in the varved lake sediments of Lago Grande di
17   Monticchio, southern Italy', Quaternary Science Reviews, 118pp. 67–83.

18   Zanchetta, G., Sulpizio, R., Giaccio, B., Siani, G., Paterne, M., Wulf, S. & D'Orazio, M. (2008) 'The
19   Y-3 tephra: A Last Glacial stratigraphic marker for the central Mediterranean basin', Journal
20   of Volcanology and Geothermal Research, 177(1), pp. 145–154.

21
22
23
24
25
26
27
28
29
30
31
32
33
34
35
36
37
38
39
40
41
42
43
44
45
46
47
48
49
50
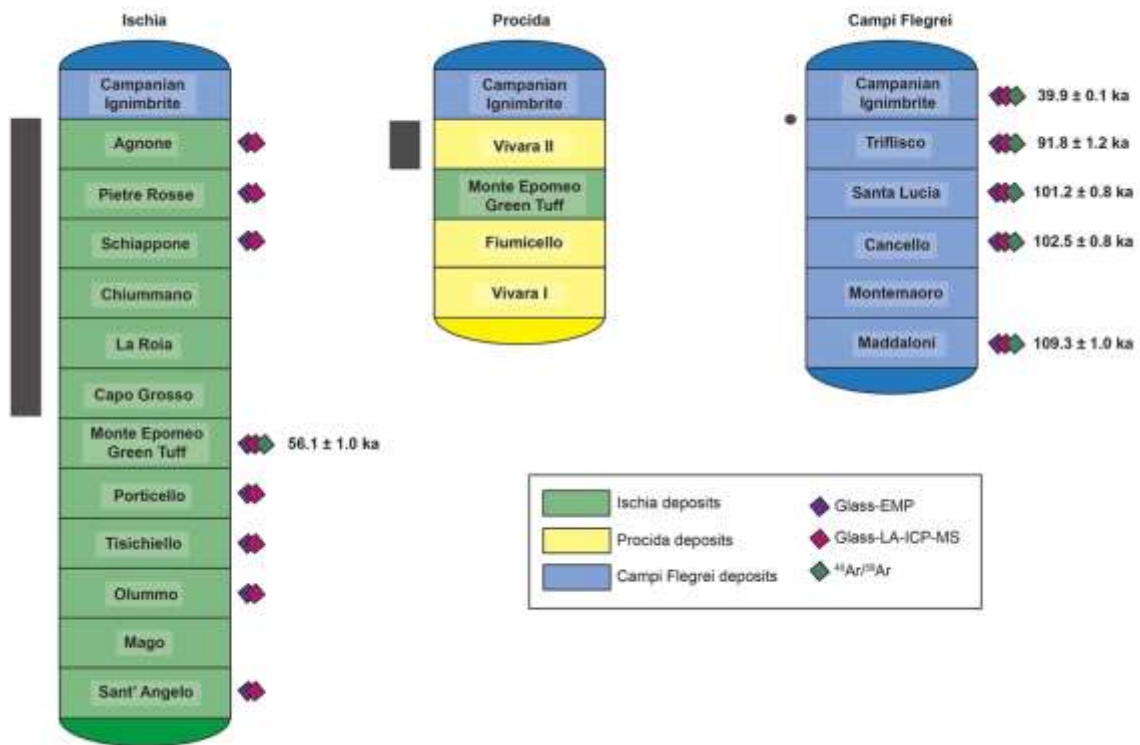
1
2 **Figure 1:** The known pre-CI eruptions from the CVZ volcanoes: Ischia (Civetta et al., 1991; Brown et
3 al., 2008); Procida (De Astis et al., 2004) and Campi Flegrei (Monaco et al., 2022). We note that these
4 are not complete stratigraphies and the timescales may very between units. Units that have major
5 element glass data (Tomlinson et al., 2012, 2014 Monaco et al., 2022), trace element glass data
6 (Tomlinson et al., 2012, 2014 Monaco et al., 2022) and $^{40}Ar/^{39}Ar$ ages (Giaccio et al., 2017; Monaco et
7 al., 2022) are marked. Grey bars and dot denote the stratigraphic position of the Acquamorta sequence
8 that is the focus of this study.
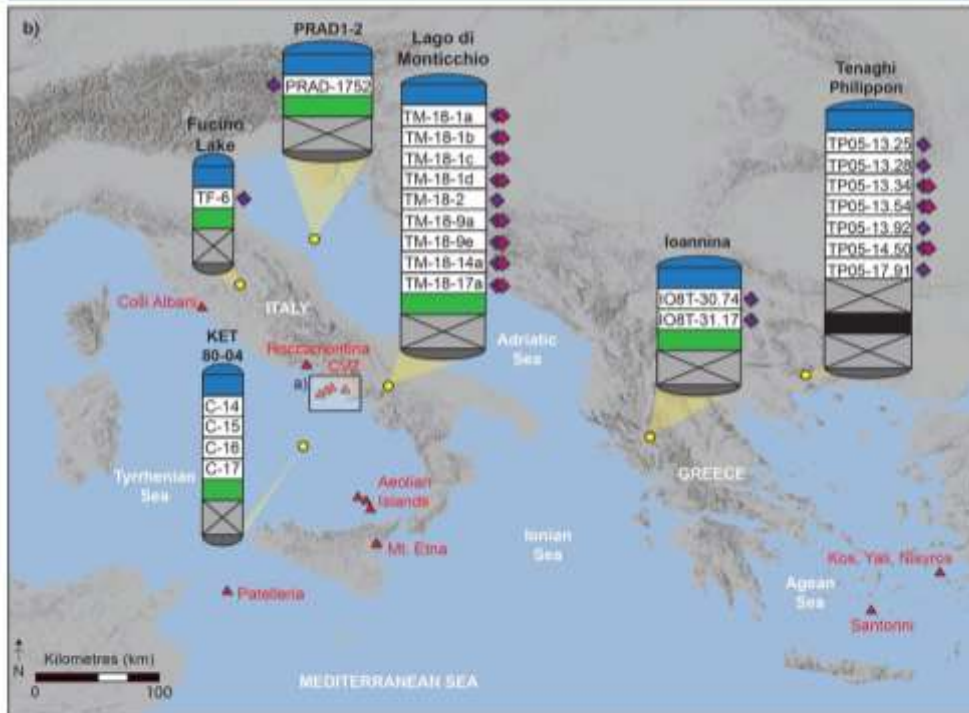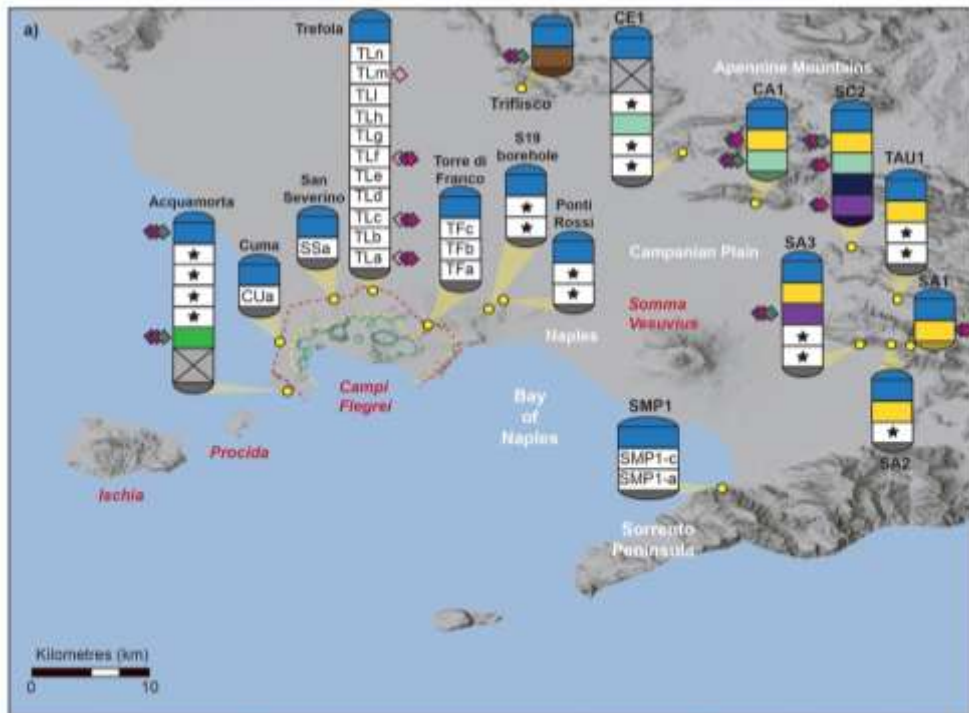
Widespread >40 ka Campi Flegrei tephra markers

- CI (39.9 ± 0.1 ka ⁴⁰Ar/³⁹Ar; Giaccio et al., 2017)
- MEGT (56.1 ± 0.1 ka ⁴⁰Ar/³⁹Ar; Giaccio et al., 2017)
- Triflisco (91.8 ± 0.1 ka ⁴⁰Ar/³⁹Ar; Monaco et al., 2022)
- Santa Lucia (101.0 ± 0.8 ka ⁴⁰Ar/³⁹Ar; Monaco et al.,
- Cancello (103.0 ± 0.8 ka ⁴⁰Ar/³⁹Ar; Monaco et al., 2022)
- X-5 (106.2 ± 1.3 ka ⁴⁰Ar/³⁹Ar; Regattieri et al., 2015)
- Maddaloni (109.3 ± 1.0 ka ⁴⁰Ar/³⁹Ar; Monaco et al.,
- X-6 (109.5 ± 0.9 ka ⁴⁰Ar/³⁹Ar; Regattieri et al., 2015)

Sites and associated units

- ★ Recognised but unlabelled tephra units
- ⊠ unlogged tephra units
- ○ sample site

Campi Flegrei caldera/crator rims

- ⋯ post-NYT caldera rims
- ⋯ NYT caldera rim
- ⋯ CI caldera rim

Analyses

- ◆ Glass LA-ICP-MS
- ◆ Glass EMP
- ◇ XRF whole-rock
- ◆ ⁴⁰Ar/³⁹Ar

Figure 2: A) Map showing the location of the Campanian Volcanic Zone (CVZ) and the Quaternary volcanic centres Ischia, Procida and Campi Flegrei. Map of the Campi Flegrei caldera and its major structures, modified from Vitale and Isaia (2014). The locations where proximal records with units that have been logged and characterised between the MEGT and CI across the Campanian Plain. Acquamorta (Rosi et al., 1988; Perrotta and Scarpati, 1994; Orsi et al., 1996; De Astis et al., 2004; Tomlinson et al., 2014); Cuma (Orsi et al., 1996); San Severino (Orsi et al., 1996); Orsi et al., 1996; Tomlinson et al., 2012); Torre di Franco (Orsi et al., 1996); Ponti Rossi (Orsi et al., 1996); S19 borehole (Albert et al., 2019; Isaia et al., 2018;); CE1 = Cervino (Di Vito *et al.* 2008); SIMP-1 (Di Vito *et al.,* 2008). Also shown are sites from the foothills of the Apennine Mountains where older (>56 ka) Campi Flegrei deposits have been identified and characterised (Di Vito *et al.,* 2008; Monaco *et al.,* 2022). Units beneath the CI that have been observed but are not labelled or correlated to others elsewhere are shown by white boxes with stars. **B)** Location of the distal records that have tephra units, with Campanian glass compositions, beneath the CI and above the X-6; Fucino (Giaccio *et al.,* 2017); Monticchio (Wulf et al., 2004; Tomlinson et al., 2015; Wutke et al., 2015); Ioannina (McGuire et al., 2022); KET80-04; PRAD1-2 (Bourne et al., 2010).

A

Fumicello
(Procida)

B-C →

E   D

B   CI

CF282
CF281
CF280

CI — yellow ash followed by lithic-rich breccia unit

AQ-13 CF282 — white ash, disturbed but laterally continuous
AQ-12 CF281 — distubed ash,with dark pods
AQ-11 CF280 — pods of ash with 1 mm pumice

C

CF279

CF278
CF277

CF276

CF275

CF274

AQ-10 CF279 — bimodal in colour with layers of both dark and light pumices.

CF278B
CF278A

AQ-9

CF277 — poorly sorted, yellow ash with some pumice, laminations and accretionary lapilli. At top there is a well sorted clast supported unit with 1-4 cm pumices (CF278A) followed by a laminated, poorly sorted ash unit (CF278B)

AQ-8 CF276 — poorly sorted, fine to coarse grey ash

AQ-7 CF275 — coarse lapilli pumice layer followed by grey ash with brown bands.

AQ-6 CF274 — thick undulating layer of white-grey coarse ash with some banding (weathering)

D

CF272

CF271
CF269   ← CF270

AQ-5 CF272 — brown-grey ash-sized reworked material followed by 10 cm thick, laterally discontinuous zone with pumices

CF271 — white unit with sub-units of pumice and ash. At the top there is clast supported, pumice lapilli unit.

AQ-4

CF270

AQ-3 CF269 — massive, white-grey, moderately-sorted fine ash unit with some small pumices. 10 cm from the base there is a band of aligned, angular pumices

AQ-2 CF268 — pods of clast supported, fine-medium sized lapilli

E   F

CF268

MEGT
CF191

50 cm

>1.7 m clast supported unit with pumices up to 10 cm in size

MEGT CF191

fine med. coarse

Lithostratigraphy

Laminated ash with lapilli
Ash
Paleosol

Breccia
Pumice
Lapilli

Figure 3: A) The Acquamorta outcrop and the positions of the four sampling sections (B-F) indicated by white boxes. Numerous tephra units are observed in this outcrop, including the Fiumicello (dashed white line) from Procida. The tephra units observed in sections B and C are located on the southern side of the exposure below the CI. **B-F)** Annotated photos of the units (AQ-2 – AQ-13) and geochemical samples (CF-prefixes) from the sampled sections along the exposure. The composite tephrostratigraphy for the Acquamorta outcrop between the MEGT and CI showing the units (AQ-prefix) and geochemical samples (CF-prefix) as well as the unit descriptions.
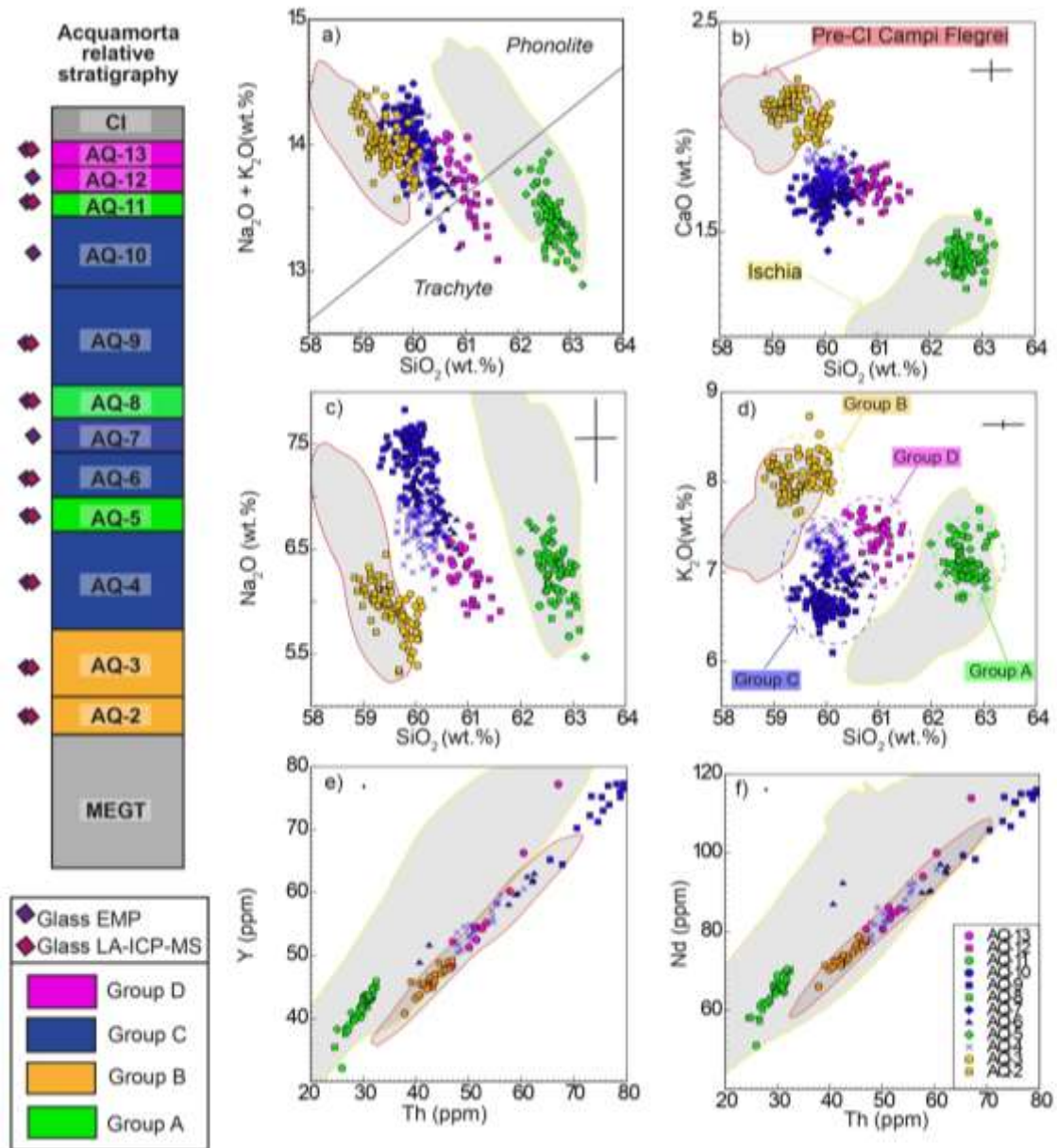
Figure 4: The relative stratigraphic order and the glass composition of the twelve tephra units at Acquamorta. Please see figure one to see how the Acquamorta stratigraphy fits into the eruption stratigraphies of the CVZ. Colours correspond to the compositional group defined using major (electron microprobe; EMP) and trace element (laser ablation inductively coupled plasma mass spectrometry; LA-ICPMS) glass compositions. **A-D)** Major and **E,F)** Trace element compositions. The limited (3 units) published Pre-CI Campi Flegrei (grey shaded area with red outline) and Ischia (grey shaded area with light green outline) glass compositions are shown as fields (Tomlinson et al., 2012, 2014, 2015). These new Group C and D have glass compositions that are consistent with Campi Flegrei, and expand the database of pre-CI glass compositions. The groups are indicated by dashed ellipses in Fig.4d. Errors are 2 s.d. calculated using replicate analyses of MPI-DING StHs6/80 glass.
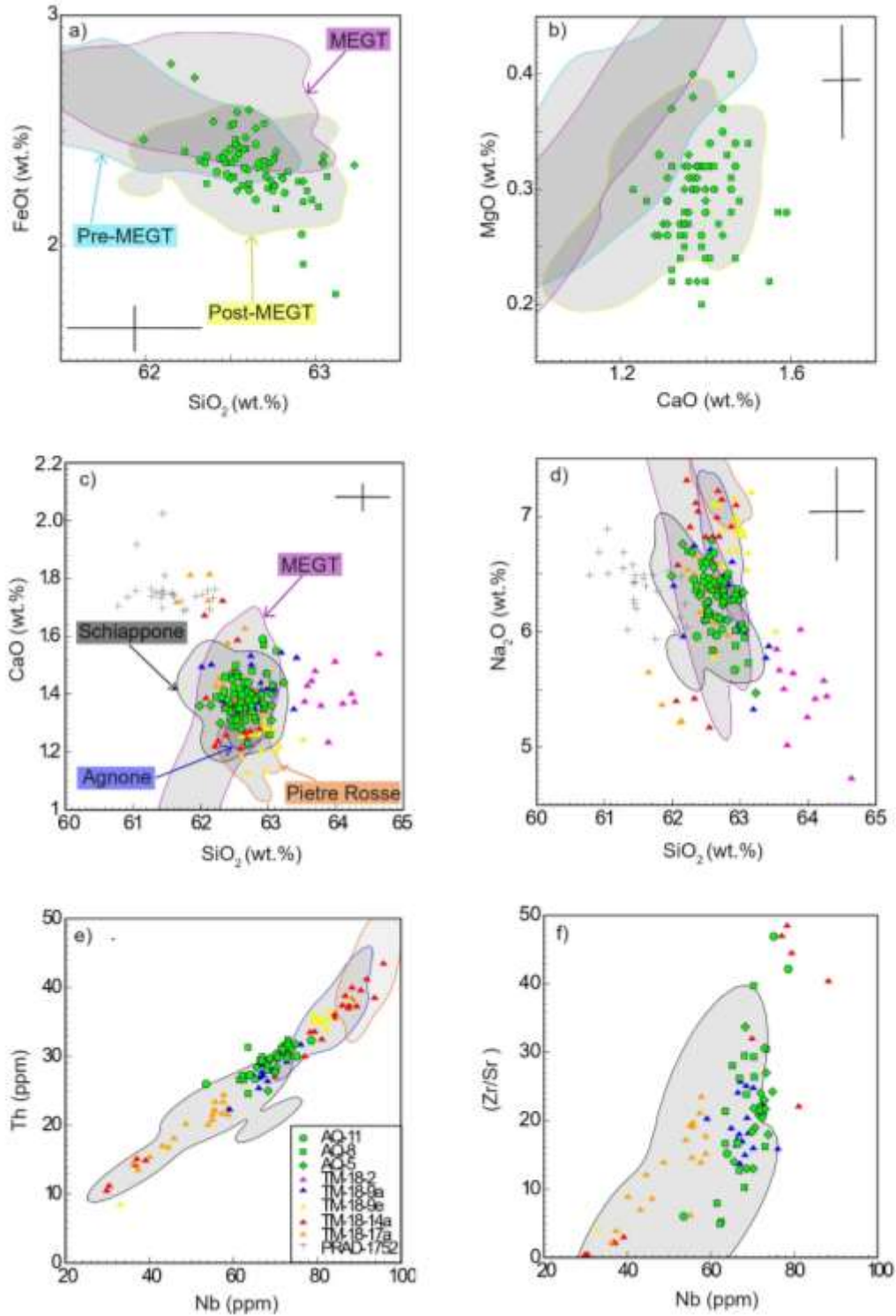
Figure 5: A,B) Glass composition of the Acquamorta Ischia layers compared to proximal glass chemistry data for pre-MEGT, MEGT and post-MEGT Ischia deposits (data from Tomlinson et al., 2014). As expected, the composition of the Acquamorta units overlap with post-MEGT deposits. **C-F)** Major **(C,D)** and trace element **(E,F)** plots of Post-MEGT Ischia units identified at Acquamorta plotted with data from the MEGT and post-MEGT Ischia eruption units (plotted as fields; Tomlinson et al., 2014), and distal tephras from LGdM (Tomlinson et al., 2014; Wutke et al., 2015) and the PRAD1-2 core (Bourne et al., 2010). Errors are 2 s.d. calculated using replicate analyses of MPI-DING StHs6/80 glass.
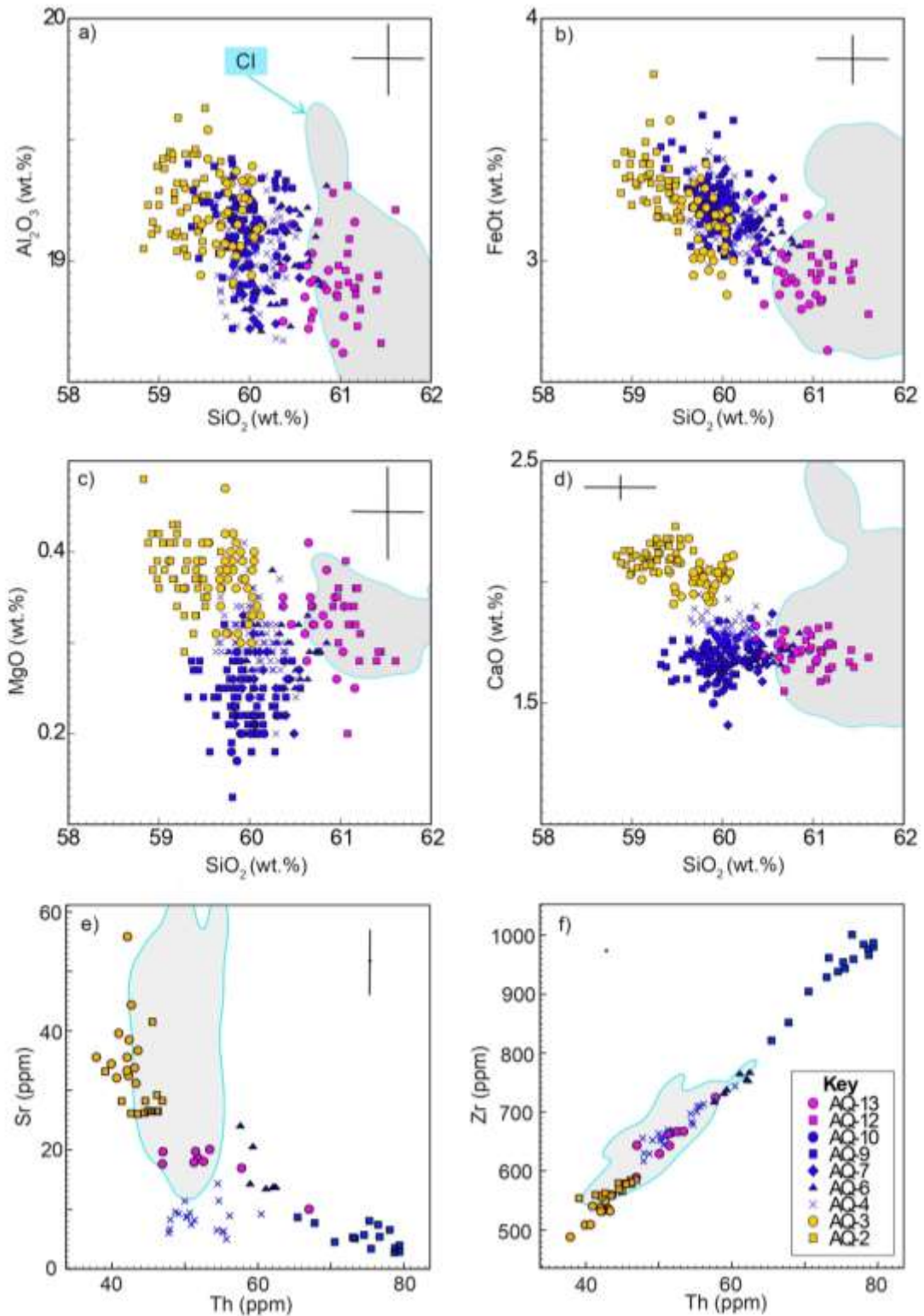
Figure 6: Major **A-D)** and trace **E,F)** element compositions of all nine pre-CI Campi Flegrei tephra units from the three compositional groups sampled at Acquamorta plotted alongside the compositional field of the CI (grey shaded area with blue outline; data from Tomlinson et al., 2012). Errors are 2 s.d. calculated using replicate analyses of MPI-DING StHs6/80 glass.
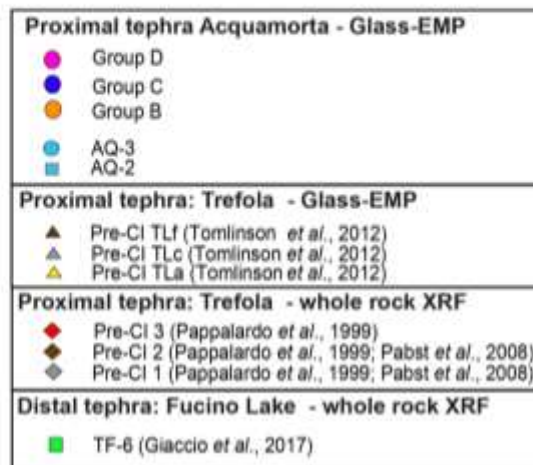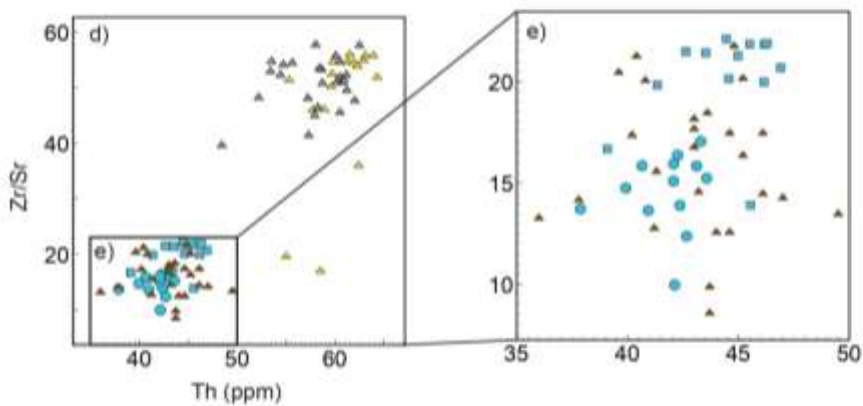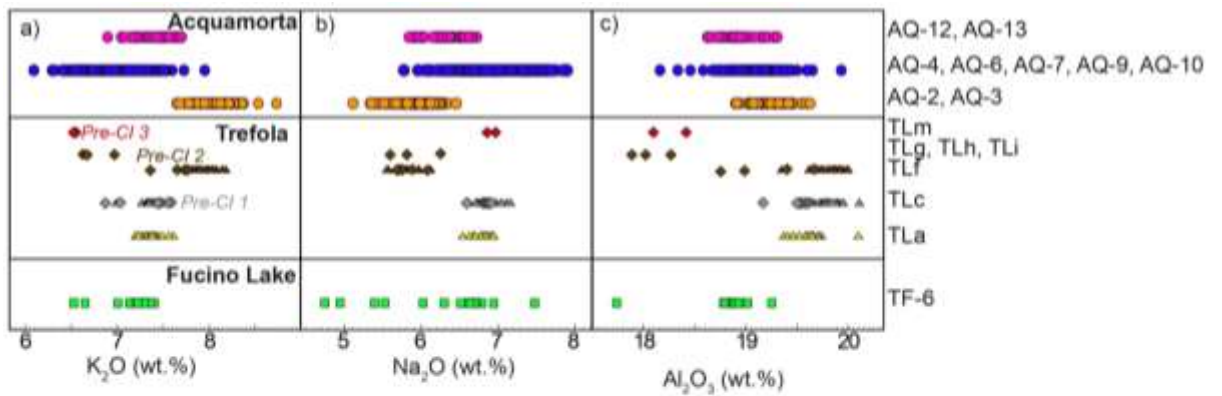
Figure 7: A-C) Major element plots of the three pre-CI Campi Flegrei compositional groups from Acquamorta alongside the units from Fucino Lake (distal) and Trefola (proximal), including three pre-CI compositional groups defined by Pabst et al., 2008. **D,E)** Trace element plots of the Group B units from Acquamorta (AQ-2 and AQ-3) with three units from Trefola (TLa, FLc and TLf). Data from: (1) XRF whole-rock (Pappalardo et al., 1999; Pabst et al., 2009) and (2) data from glass shards (Tomlinson et al., 2012; Giaccio et al., 2017).

Figure 8: A,B) Major element plots of the Acquamorta Group D tephras (AQ-12 ad AQ-13) with the four tephras found directly beneath the CI in the LGdM sequence (TM-18-1a, TM-18-1b, TM-18-1c and TM-18-1d; (Wutke et al., 2015), two cryptotephras between the Y6 and the CI from the Ioannina site (I08-30.74 and I0831.17; McGuire et al., 2022), and six tephras between 40,670 - 47,310 cal yr BP from Tenaghi Phillippon (Wulf et al., 2018). The field for the CI upper flow (red field), CI lower and intermediate flow (grey field) and the CI fall deposits (green field) is obtained from the literature (Tomlinson et al., 2012). **C-F)** Trace element of the Group D tephra units (AQ-12 and AQ-13) at Acquamorta with the four tephras found directly beneath the CI in the LGdM sequence (TM-18-1a, TM-18-1b, TM-18-1c and TM-18-1d; (Wutke et al., 2015) alongside the data of the CI deposits (Tomlinson et al., 2012). Errors are 2 s.d. calculated using replicate analyses of MPI-DING StHs6/80 glass.

Table 1: EMP and LA-ICP-MS of representative analysis shards from the deposits preserved between the MEGT and CI identified in this study. It should be noted that n is the size of the population from which the representative analysis was selected.

Tephra unit	AQ-13	AQ-12	AQ-11	AQ-10	AQ-9	AQ-9	AQ-9	AQ-8	AQ-7	AQ-6	AQ-5	AQ-4	AQ-4	AQ-4	AQ-3	AQ-2
Sample	CF282	CF281	CF280	CF279	CF278A	CF278B	CF277	CF276	CF275	CF274	CF272	CF271	CF192	CF270	CF269	CF268
Compositional Group	Group D	Group D	Group A	Group C	Group C	Group C	Group C	Group A	Group C	Group C	Group A	Group C	Group C	Group C	Group B	Group B
(wt.%)																
SiO_2	60.71	61.22	62.53	59.91	59.98	59.65	59.70	62.52	59.92	60.02	62.65	60.29	59.68	60.26	59.76	59.31
TiO_2	0.42	0.43	0.48	0.46	0.46	0.41	0.41	0.45	0.42	0.47	0.47	0.40	0.50	0.44	0.42	0.41
Al_2O_3	18.92	18.80	18.61	19.13	19.08	19.27	18.93	18.78	18.97	18.92	18.44	18.68	18.88	18.90	19.20	19.22
$FeOt_t$	2.91	2.98	2.38	3.22	3.12	3.06	3.30	2.30	3.15	3.18	2.51	2.94	3.14	3.18	3.34	3.34
MnO	0.23	0.23	0.18	0.33	0.29	0.31	0.26	0.15	0.34	0.20	0.17	0.30	0.22	0.22	0.17	0.20
MgO	0.32	0.31	0.34	0.20	0.29	0.24	0.25	0.26	0.25	0.27	0.32	0.32	0.35	0.27	0.31	0.39
CaO	1.73	1.74	1.47	1.65	1.74	1.70	1.69	1.35	1.72	1.79	1.35	1.81	1.83	1.75	2.00	2.12
Na_2O	6.35	6.23	6.26	7.46	7.18	7.31	7.60	6.26	7.08	6.92	6.31	6.85	6.98	6.52	5.58	6.12
K_2O	7.61	7.30	7.21	6.64	6.70	6.87	6.67	7.16	7.04	7.12	7.03	7.38	7.32	7.35	8.17	7.85
P_2O_5	0.03	0.05	0.02	0.05	0.00	0.05	0/06	0.09	0.02	0.06	0.07	0.0	0.06	0.00	0.06	0.04
Cl	0.77	0.71	0.52	0.96	1.15	1.14	1.14	0.69	1.08	1.05	0.67	0.95	1.02	1.09	0.98	0.99
Analytical total	95.87	96.54	95.27	95.08	96.70	97.84	96.41	96.92	97.02	97.25	96.67	97.63	94.92	98.68	95.99	94.13
(n)	17	21	18	15	33	24	8	30	21	31	23	41	4	26	46	39
(ppm)																
Rb	465	-	361	-	583	587	-	356	-	472	353	462	469	-	407	418
Sr	18.6	-	24.8	-	5.28	3.96	-	32.3	-	13.7	21.9	6.49	6.67	-	38.5	26.5
Y	54.4	-	40.2	-	72.2	77.3	-	41.1	-	61.6	43.2	57.1	50.5	-	45.6	48.1
Zr	665	-	414	-	929	987	-	411	-	755	446	697	617	-	535	578

Nb	120	-	66.5	-	177	178	-	66.9	-	142	72.3	131	121	-	102	111
Ba	11.8	-	14.7	-	1.83	1.46	-	29.6	-	11.3	15.0	8.01	3.67	-	12.0	7.70
La	127	-	85.6	-	170	179	-	88.0	-	143	89.8	135	119	-	109	116
Ce	243	-	166	-	330	342	-	170	-	273	178	259	231	-	207	223
Pr	24.3	-	17.7	-	32.0	34.0	-	18.0	-	27.1	18.5	25.9	22.8	-	20.9	22.2
Nd	84.6	-	64.7	-	108	116	-	66.0	-	95.5	65.2	88.0	77.7	-	72.7	77.7
Sm	14.6	-	11.8	-	18.4	19.5	-	12.0	-	16.5	12.0	15.6	13.6	-	12.8	13.0
Eu	1.35	-	1.46	-	1.21	1.29	-	1.37	-	1.35	1.37	1.41	1.17	-	1.75	1.67
Gd	10.7	-	9.33	-	15.2	16.2	-	8.98	-	12.2	9.44	12.8	``.0	-	10.0	10.5
Dy	9.80	-	7.39	-	13.0	14.1	-	7.78	-	10.9	8.13	10.5	9.53	-	8.26	8.92
Er	5.56	-	3.95	-	7.65	8.28	-	4.12	-	6.30	4.45	5.76	4.89	-	4.45	4.83
Yb	5.59	-	4.03	-	7.79	8.45	-	4.24	-	6.78	4.56	5.73	4.82	-	4.64	5.03
Lu	0.81	-	0.62	-	1.15	1.19	-	0.62	-	0.93	0.67	0.84	0.74	-	0.68	0.74
Hf	14.3	-	9.44	-	19.5	20.7	-	9.20	-	16.6	10.4	14.5	13.0	-	11.4	12.5
Ta	5.68	-	3.39	-	8.22	8.62	-	3.47	-	6.78	3.72	6.11	5.45	-	4.80	5.25
Pb	64.8	-	50.3	-	86.3	75.6	-	45.2	-	71.2	49.3	67.8	77.7	-	62.3	62.0
Th	51.8	-	29.5	-	73.0	79.4	-	29.3	-	62.1	31.1	54.4	47.9	-	42.4	46.2
U	18.6	-	9.04	-	27.4	28.6	-	9.27	-	21.7	10.0	19.5	18.0	-	14.7	16.8
(n)	11	-	5	-	6	9	-	16	-	9	11	7	12	-	13	13